UNIVERSIDADE DE LISBOA
FACULDADE DE CIÊNCIAS
DEPARTAMENTO DE BIOLOGIA VEGETAL

Development of novel bacterial enzymes for medical diagnosis through directed evolution

André Filipe Teixeira Taborda

Mestrado em Microbiologia Aplicada

Dissertação orientada por:
Prof. Lígia O. Martins
Prof. Ana Tenreiro

2019

This Dissertation was fully performed at Instituto de Tecnologia Química e Biológica – ITQB Universidade Nova de Lisboa under the direct supervision of Professor Lígia O. Martins

Professor Ana Tenreiro was the internal supervisor designated in the scope of the Master in Applied Microbiology of the Faculty of Sciences of the University of Lisbon

Acknowledgments

Na última etapa deste ciclo, que culmina com a entrega desta dissertação de tese de mestrado, queria nomear e sobretudo agradecer a todos os que de forma direta ou indireta contribuíram para a sua realização.
Em primeiro lugar gostaria de agradecer ao laboratório Microbial and Enzyme technology (ITQB) a disponibilidade em me terem aceite assim como os recursos que me forneceram para que pudesse realizar todo o trabalho laboratorial e ainda a possibilidade de estar presente nalguns seminários e conferências que ajudaram a complementar a minha formação.
A todos os investigadores e alunos do laboratório assim como do gabinete em que me encontrava o meu obrigado pela troca de ideias e desabafos sempre que necessário.
Em particular, o meu grande agradecimento à professora Lígia Martins, orientadora deste trabalho, por ser das pessoas mais focadas, dinâmicas, dedicadas e trabalhadoras que já conheci, tentando estar presente em todas as decisões experimentais e motivando sempre que os resultados não foram tão animadores. É, indubitavelmente, um exemplo a seguir. Pode ter a certeza que contribuiu para o meu percurso como investigador/cientista.
À Doutora Vânia Brissos, por todos os conselhos fornecidos durante o decorrer do trabalho experimental que foram essenciais para o seu sucesso.
À professora Teresa Catarino pela disponibilidade e conhecimento que foram importantes na obtenção das cinéticas por Stopped-flow.
À Mariana Lima, aluna de licenciatura que frequentou o laboratório no âmbito do seu projeto de curso ajudando na otimização da produção em larga escala assim como na obtenção de alguns dados de Stopped-flow.
Às técnicas do ITQB Teresa Silva e Isabel Pacheco pela disponibilidade, ajuda e formação na execução de alguns procedimentos experimentais.
E finalmente a toda a minha família e amigos, evidenciando especialmente os meus pais, pela ajuda que demonstraram ao longo de toda a minha formação, apoiando e motivando sempre.
Obrigado!

Abstract

Pyranose 2-oxidases (P2Oxs) have a great potential to replace the typical glucose oxidases (GOxs) and glucose dehydrogenases (GDHs), specific for β-D-glucose anomer, in glycemia monitoring biosensors. P2Oxs are flavoenzymes mostly identified in Fungi that catalyzes the regioselective oxidation of C2 alcohol moiety of several aldopyranoses originating the correspondent keto-sugar with the concomitant reduction of O_2 to H_2O_2. The use of O_2 as cheap and clean oxidant and in particular the lack of D-glucose anomer preference represent very attractive points for the biotechnological application of P2Oxs. In this work, directed evolution (DE) methodologies were applied to improve the first identified bacterial P2Ox, from *Pseudoarthrobacter siccitolerans*, AsP2Ox, in its specificity and activity for D-glucose. This strategy was supported by transient-state analysis in combination with oxygen consumption steady-state kinetics showing that the reductive half-reaction (oxidation of D-glucose) is the limiting step of the catalytic mechanism. We first optimized and validated colorimetric screening enzymatic assays based on 'activity-on-plate' and 96-well plates using cell crude extracts. These screenings allowed analyze in a high-throughput mode, thousands of variants generated by error-prone PCR. The hit variant from the first-generation 1A1 harbors only one mutation, G366S, located close to the substrate binding site. Biochemical and kinetic analysis using purified enzyme showed that 1A1 has a 2-fold increased k_{cat} (turnover number) and 2-fold higher protein production yields as compared with the wild type enzyme. In a second round of directed evolution a new hit variant 5D5 was selected, carrying four additional mutations (S22S, A75T, A206T, Q295H). The pH profile of 5D5 revealed an optimum pH shifted 1 unit towards the alkaline range, a 6-fold higher k_{cat} and 3-fold production yields than the wild-type enzyme. The analysis of mutations using site-directed mutagenesis showed that both G366S and Q295H are key mutations, which under an epistatic effect contributed to the higher catalytic efficiency exhibited by 5D5 hit variant. The comparison of kinetic parameters of 5D5 variant with GOxs and GDHs show that its K_m remains too high and the k_{cat} too low in order to replace the traditional enzymes in biosensors. Therefore, the evolution of AsP2Ox must continue using 5D5 as the parent in new rounds of DE to achieve an improved variant exhibiting the properties that fit the desired application.

key-words: Biosensors, Flavoproteins, Pyranose 2-oxidase, Laboratory enzyme evolution, High-throughput screening.

Resumo

Piranoses 2-oxidases (P2Oxs) são enzimas que oxidam açúcares, nomeadamente D-glucose, no carbono C2, o que representa uma vantagem na substituição das atuais enzimas usadas em biossensores para monitorização da glicemia, as glucose oxidases (GOxs) e glucose desidrogenases (GDHs), que apenas oxidam no carbono C1, o anómero β-D-glucose. Como consequência, o uso das P2Oxs em biossensores poderá conduzir a uma medição mais sensível dos níveis de D-glucose no sangue.

As P2Oxs são flavoenzimas que foram identificadas maioritariamente em fungos com funções relacionadas com a degradação da biomassa vegetal. Estas enzimas catalisam a oxidação seletiva do grupo álcool do carbono C2 de diversas aldopiranoses originando as respetivas ceto-piranoses. Como aceitador de eletrões, estas enzimas podem utilizar um vasto repertório de moléculas (como quinonas e radicais) mas a sua grande vantagem reside na utilização de oxigénio molecular, que é um oxidante barato e "limpo", que é reduzido a peróxido de hidrogénio durante o seu ciclo catalítico. Este divide-se em duas semirreações, uma redutiva, relacionada com a redução do cofator FAD a $FADH_2$ em consequência da oxidação do carbono C2 dos açúcares libertando como produto, o respetivo ceto-açúcar, e uma oxidativa, associada à reoxidação do $FADH_2$ a FAD, na presença de um aceitador de eletrões, como o dioxigénio.

Atualmente, para além das P2Oxs fúngicas, três P2Oxs de origem bacteriana foram caracterizadas entre as quais se destaca a AsP2Ox, da bactéria *Pseudoarthrobacter siccitolerans* por ter sido a primeira e cuja identificação foi realizada no laboratório de Tecnologia Microbiana e Enzimática do ITQB NOVA. A caracterização desta enzima revelou, no entanto, uma baixa afinidade para a D-glucose. Assim, este trabalho de dissertação teve como principal objetivo a aplicação de técnicas de evolução dirigida (DE) para melhorar a enzima AsP2Ox de modo a aumentar a sua especificidade e atividade para o uso da D-glucose como substrato de modo a que possa ser empregue em biossensores de monitorização da glicemia. Esta estratégia de engenharia foi eleita, uma vez que a ausência de uma estrutura cristalina da enzima ou de um modelo estrutural fidedigno, não é possível fazer previsões de melhoramento racional baseado em relações entre a estrutura e a função.

A engenharia de enzimas por Evolução Dirigida requer a otimização de um número de parâmetros desde o crescimento das estirpes recombinantes, métodos de rutura celular até ao rastreio de atividade enzimática. Neste trabalho desenvolveu-se, otimizou-se e validou-se duas metodologias para rastreios em larga escala *(high-throughput screenings)* que possibilitaram a análise de alguns milhares de variantes gerados por *error-prone* PCR nas duas gerações de evolução dirigidas efetuadas. Uma das metodologias utilizou como alvo colónias de células em placa de Petri ('*activity-on*-plate') e outra, extratos celulares brutos, após crescimento das colónias em meio líquido em placas com 96 poços. Uma das otimizações realizadas foi no método de deteção da atividade enzimática da AsP2Ox. Sendo o oxigénio molecular o aceitador final de eletrões pretendido, a atividade da enzima é medida através de uma reação acoplada utilizando uma peroxidase (*e.g.* Horseradish peroxidase, HRP), que consume o peróxido de hidrogénio formado pela AsP2Ox e oxida um substrato que origina um produto corado, cuja formação possa ser facilmente monitorizada num espectrofotómetro. Provou-se que o ABTS, substrato da HRP mais comumente utilizado neste tipo de reações acopladas, levava a medições subestimadas de atividade da AsP2Ox. Por conseguinte, testou-se um novo sistema de substratos baseado em dois compostos (AAP e DCHBS) que, por atividade da HRP e na presença de H_2O_2 origina um composto cor-de-rosa, doseado espetrofotometricamente a 515 nm que se revelou um método mais adequado para seguir a atividade da AsP2Ox.

As biblioteca de variantes geradas por "*error-prone PCR"* foram rastreadas num primeiro passo através da metodologia *'activity-on-plate'*, que sendo qualitativa, permitiu identificar clones com atividade e diminuir o número de variantes a serem avaliados com maior rigor. O segundo *screening,* em placas de

96 poços, com carácter quantitativo, necessitou de ser exaustivamente otimizado de modo a diminuir o risco de se selecionar falsos positivos. Assim, observou-se que o uso da estirpe KRX de *E. coli* como estirpe de expressão da proteína de interesse, em placas de 96 poços de poços fundos e consequente disrupção dos pellets celulares recorrendo a lisozima era a combinação que conduzia a um coeficiente de variação (CV) para a atividade total da AsP2Ox menor, sendo por isso, aplicado na avaliação dos variantes selecionados por *'Activity-on-plate'*.

Na primeira geração de DE, dos 7300 variantes analisados em *'Activity-on-plate'*, cerca de 100 foram inoculadas em placas de 96 poços de poços fundos e sujeitos a *screenings*, o que permitiu a identificação de um variante, 1A1, que continha uma mutação na posição 366 (glicina para serina), a cerca de 10 Å do N5 do cofator FAD e cuja atividade relativa ao wild-type era de 3.7 ± 0.9 (em extratos celulares brutos). Posteriormente, numa segunda geração de DE, dos cerca de 900 variantes pré-selecionados para análise em placa de 96 poços, um, denominado de 5D5, apresentou atividade enzimática melhorada obtendo uma atividade relativa ao parente (1A1) de 5.0 ± 0.9. Os resultados da sequenciação do variante 5D5 revelaram a existência de 4 mutações adicionais, sendo uma delas sinónima (S22S), duas localizadas na superfície da enzima (A75T e A206T) e uma (Q295H) dentro da suposta cavidade de ligação ao substrato distando cerca de 11 Å do N5 da molécula de FAD.

A análise dos dois variantes obtidos durante a DE, após crescimento em escala grande e purificação, revelou que 1A1 apresenta um aumento nos níveis de produção da enzima (cerca de duas vezes) assim como do parâmetro k_{cat} de duas vezes quando comparado com o wild-type. Já o mutante da segunda geração, 5D5, mostrou um desvio do pH ótimo de 7.5 para 8.5, um ligeiro aumento na produção de proteína funcional, e uma melhoria notória do k_{cat} 6 vezes superior em relação ao wild-type, apresentando uma eficiência catalítica de 3.22 ± 0.39 M^{-1} s^{-1}.

De modo a contribuir para o conhecimento sobre o mecanismo catalítico da AsP2Ox utilizou-se um aparelho de *stopped-flow* para determinar as constantes de segunda ordem das semirreações redutiva e oxidativa da AsP2Ox. Os resultados indicaram que a semirreação redutiva apresenta uma velocidade 6 ordens de magnitude mais lenta do que a semirreação oxidativa, fazendo com que o passo limitante do ciclo catalítico seja a oxidação da D-glucose justificando que o seu melhoramento seja um dos principais objetivos deste trabalho. A técnica de *stopped-flow* (seguindo a semirreação redutiva) e ainda cinéticas medindo diretamente o consumo de oxigénio num Oxygraph® permitiram ainda suportar os dados de estado estacionário garantindo que a evolução da proteína desde o wild-type até ao variante 5D5 foi bem sucedida.

Finalmente, de modo a tentar entender o papel das mutações que foram introduzidas durante o processo evolutivo, recorreu-se à técnica de mutação dirigida para originar os mutantes simples (A75T, A206T e Q295H) e o mutante duplo (Q295H/G366S) que permitiu concluir que as mutações Q295H e G366S, que distam ~7 Å entre si, estão sob um efeito epistático envolvido na melhoria da atividade obtida no variante 5D5, uma vez que o efeito das duas mutações conjuntas é superior ao efeito individual de cada uma das mutações. Adicionalmente, concluiu-se que a mutação Q295H era a responsável pelo desvio de pH ótimo verificado no variante da ultima geração e que as mutações A75T e A206T, embora não desempenhem um papel ativo na melhoria cinética, podem estar relacionadas com os melhores rendimentos de produção proteica obtidos no ultimo variante.

Uma comparação dos parâmetros cinéticos (estado estacionário) do último variante obtido, 5D5, com os das GOXs e GDHs, sugere que o K_m da AsP2Ox permanece alto e o k_{cat} baixo o que invalida, por enquanto, a sua aplicação em biossensores de rastreio da glicemia, motivando assim o grupo de investigação a continuar a evolução desta proteína, partindo do variante 5D5 como parente para novas rondas de evolução dirigida, de modo a encontrar uma enzima que cumpra os requisitos para a desejada aplicação.

Palavras-chave: Biosensores, Flavoproteinas, Piranose 2-oxidase, Evolução dirigida, Análise *high-through put*.

List of contents

Figures index

Tables index

Abbreviations list

1,5-AG	1,5-anhydro-D-glucitol
AAP	4-Aminophenazone
Abs	Absorbance
ABTS	2,2'-azino-bis (3- ethylbenzothiazoline-6-sulfonic acid)
AsP2Ox	*Arthrobacter siccitolerans* pyranose 2-oxidase
B-PER	Bacterial Protein Extraction Reagent
CV	Coefficient of variance
DE	Directed evolution
DCHBS	3,5-Dichloro-2-hydroxybenzene-sulfonic acid
DCPIP	2,6-Dichlorophenolindophenol
dNTPs	Deoxyribonucleotide triphosphate
epPCR	Error prone polymerase chain reaction
FACS	Fluorescence-activated cell sorting
FAD	Flavin adenine dinucleotide
GDH	Glucose dehydrogenase
GMC	Glucose-methanol-choline
GOx	Glucose oxidase
HPLC	High Performance Liquid chromatography
HRP	Horseradish peroxidase
IPTG	Isopropyl β-D-1-thiogalactopyranoside
IVC	*in vitro* compartmentalization
LB	Luria-Bertani
NMR	Nuclear magnetic resonance spectroscopy
OD_{600nm}	Optical density at 600 nm
P2Ox	Pyranose 2-oxidase
PCR	Polymerase chain reaction
Pink chromogen	N-(4-antipyryl)-3-chloro-5-sulfonate-p-benzoquinone-monoimine
RT	Room temperature
SDS-PAGE	Sodium dodecyl sulfate polyacrylamide gel electrophoresis
SOB	Super Optimal Broth
SDM	Site-directed mutagenesis
SSM	Site-saturation mutagenesis
TB	Terrific Broth
Tris	Tris (hydroxymethyl)aminomethane
UV-Vis	Ultraviolet-Visible
WT	Wild-type

1. Introduction

1.1 Overview on biosensors

Biosensorics, the science of biosensors, represents a branch of biotechnology arising in the 20th century as a result of symbiotic contributions from biology, biophysics, chemistry, physics, electronics, and informatics [1].

Biosensors are analytic systems constructed to detect an analyte whereas the analyzer is from a biological source [1]. On the backstage of an analyzer, a more or less developed electronic system transduce the biosensor activity in electric current to produce a quantitative signal [2]. Biosensors are developed from biological material such as antibodies or nucleic acids but the most extensively studied are the enzyme-based biosensors, in some cases, the use of whole cells as biosensors as a base of the immobilized biocatalysts proved to be advantageous originating the cell-based biosensors in which the microbial biosensors are common [2].

The microbial biosensors are mostly used in the environmental biotechnology branch and their advantages are due to the simplicity of microbial cultivation, high analytical prospects, and reliability. In these biosensors the microorganism can be seen as a complex "bag of intracellular enzymes" where the analyte crosses microbial cells, are metabolized by intracellular enzymes (where the co-substrates are consumed) and reaction products are generated (frequently they are electrochemically active). However, the major challenges for the use of this type of biosensors relies on the selection of a microorganism that allow for high substrates specificity (high selectivity) and enough sensitivity of products detection [1].

Enzyme-based biosensors show a broad range of applications and are considered a key focus of research in the area. The advantages related with their utilization are due to the usual high specificity of enzyme-substrate interactions and the high turnover rates of biocatalysts without the interference of intracellular metabolism (as is the case in microbial-based biosensors). The basics in enzyme-based biosensors is the ability to detect the presence of certain analytes by measuring changes (*e.g.* proton concentration) that occurred during the substrate consumption (or product formation) by the enzyme. The challenging steps in the development of enzyme biosensors are in the improvement of the biocatalyst sensitivity to produce a signal at lower concentrations of the analyte, and robustness, that lead to the optimization of immobilization processes [2].

1.2 Enzyme-based biosensors to measure D-glucose concentration

One of the most popular applications of enzyme-based biosensors is the measurement of carbohydrates in samples, in particular the monitoring of glycemic levels in blood [3].Glucose sensors were evolved to adapt to the desired functions and properties and currently they are categorized in three different generations distinguishable by the final electron acceptors used. In first-generation, the electron acceptor is dioxygen that is reduced to H_2O_2 that can further transfer the electrons to the electrode. In the second-generation some mediators are used, replacing the O_2 utilization. In the third-generation the mediators are eliminated and the enzyme can transfer directly the electrons to the electrode avoiding error introduced, by *e.g.* the oxygen concentration in samples (Figure 1.1) [3]. These biosensors are mainly based in the action of Glucose oxidases (GOxs) and Glucose dehydrogenases (GDHs), responsible for the C1 oxidation of D-glucose but can be distinguished by the capability of using (GOXs) or not (GDHs) dioxygen as electron acceptor. Both GOxs and GDHs show advantages and disadvantages, for example,

GOxs showed are in general more specificity for β-D-glucose while GDHs show higher activity. These properties can be typically improved by protein engineering [3].
Recently, others carbohydrate-using enzymes, namely, Pyranose-2-oxidases (P2Oxs), are being considered as biosensors for determine glycemic levels in blood. Unlikely GOxs or GDHs, that catalyses the oxidation of D-glucose in C1 which is susceptible of anomers distinction using the β-D-glucose, P2Ox shows a major advantage of acting on the C2 alcohol moiety which makes both, α- and β-D-glucose anomers, susceptible of enzymatic oxidation leading in improved sensitivity during the response time [4], [5].

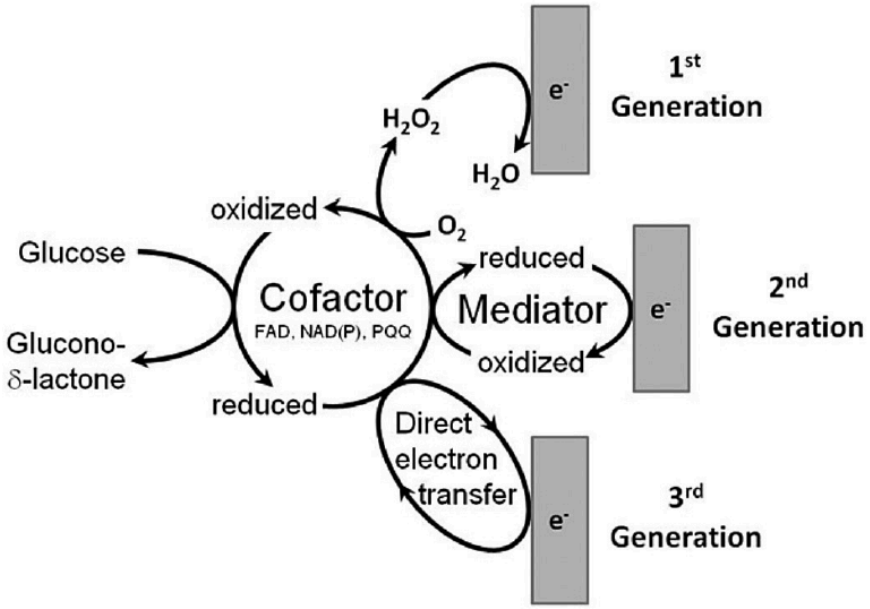

Figure 1.1 Schematic representation of three generations D-glucose biosensors. In the first generation, the electrons from enzymes are transferred to dioxygen that become reduced and further transfer the electrons to the electrode, in the second generation, the electron acceptors are external mediators and in the third generation, the electrons are transferred directly to electrode. Figure taken from [3].

The substrate specificity of P2Ox is broader when compared with GOXs and GDHs, and P2Oxs were reported to use 1,5-anhydro-D-glucitol (1,5-AG) as substrate allowing the determination of the concentration of this natural D-glucose analogue in human cerebrospinal fluid and serum [6], [7]. 1,5-AG is in the bloodstream, being provided from diet but also from liver. When the levels of blood glucose are normal 1,5-AG is filtered and reabsorbed by kidneys but in hyperglycemia episodes, glycosuria blocks the reabsorption of 1,5-AG which leads to decreased levels of this metabolite in blood. This makes 1,5-AG a marker to access the glycemic control in diabetes *mellitus* [6], and Glycomark®, that allows the measurement of 1,5-AG levels is already available in the market. In this device, P2Ox oxidizes 1,5-AG releasing H_2O_2 that is quantified through a coupled horseradish peroxidase (HRP) assay that gives indirectly assess to the levels of 1,5-AG on the samples. As P2Ox can also react with D-glucose, a pre-treatment of the sample with a Glucokinase is applied to phosphorylate D-glucose that will no longer be a P2Ox substrate [8].

1.3 Pyranose 2-oxidase: General properties, Catalytic mechanism, and activity assays

Pyranose 2-oxidases (P2Ox, pyranose:oxygen 2-oxidoreductase; EC 1.1.3.10; synonym, glucose 2-oxidase) are members of the glucose-methanol-choline (GMC) oxidoreductase superfamily of enzymes [9]. This superfamily includes enzymes such as glucose oxidase, choline oxidase, cholesterol oxidase, cellobiose dehydrogenase, aryl-alcohol oxidase and pyridoxine 4-oxidase that oxidizes an alcohol moiety to the corresponding aldehyde [10]. P2Oxs contain a flavin adenine dinucleotide (FAD) molecule as prosthetic group and therefore the typical UV-Vis absorption spectra of oxidized holoenzymes show two characteristic bands at ~ 390 nm and ~ 460 nm. The 460 nm maximum of absorption is responsible for the yellow color of oxidized form of the enzyme. In accordance, the reduced holoenzymes loses this band and the protein turns colorless [11], [12]. The P2Oxs were found in Eubacteria and Fungi with some different properties.

The catalytic cycle of P2Ox, as all oxidoreductases, requires a molecule with sufficiently negative redox potential to act as an electron donor and at the end of the catalytic cycle, the presence of a molecule with a redox potential to act as an electron acceptor. As a result, the reaction can be divided into two distinct half-reactions. In the first reductive half-reaction , the electron donor (sugar) transfer two electrons to the cofactor FAD that becomes reduced ($FADH_2$) and in the second oxidative half-reaction, the $FADH_2$ transfers two electrons to an acceptor (*e.g.* dioxygen) and the enzyme turn-over ends [10] (Figure 1.2).

Several aldopyranoses and some disaccharides are reported to act as electron donors of P2Oxs including D-glucose, D-galactose, D-mannose, D-arabinose, D-fructose, L-sorbose, D-xylose, D-fucose, maltose, and trehalose but in all described non-engineered P2Ox the D-glucose is the preferred electron donor substrate [4], [10], [13], [14]. The oxidation of these pyranoses occurs regioselectively in the C2 position releasing a sugar in the 2-keto-aldopyranose form [4], [14], [15]. In the literature, it was reported that some sugars can be also oxidized to a smaller extent at carbon C3 [16] and, in other cases, the C3 oxidation by P2Ox occur as a side reaction in substrates whereas the C2 hydroxyl group is compromised (*e.g.* when 2-deoxy-D-glucose was used as substrate) [17], [18].

In the oxidative half-reaction, these enzymes use O_2 as final electron acceptor which releases H_2O_2 as co-product of the reaction but some quinones (as *para*-benzoquinone), substituted quinones (*e.g.* DCPIP), complexed metal ions (*e.g.* ferrocenium and manganese complexes) and radicals (*e.g.* radical cation $ABTS^{\bullet+}$) were reported to also act as final electron acceptors of the P2Ox redox cycle [19]. Interestingly, in the oxidative half-reaction when O_2 is used as substrate, it was observed, for the first time, the formation of a C-4a-hydroperoxyflavin intermediate [20] which is an intermediate barely detected in other oxidases due to the spatial constraints that bypass this intermediary step [21].

Considering the redox cycle described, the methodologies that have been used to follow the reaction progress of these enzymes include UV-Vis absorbance, HPLC and NMR that measure the reduced or oxidized sugar forms in a time-course manner [22]–[24]. UV-Vis is the most common technique and has been used to follow the reduced/oxidized final acceptor (*e.g.* at 290 nm to follow hydroquinone formation, the reduced form of *para*-benzoquinone) [19] or when dioxygen is used as a final electron acceptor, a reaction coupled assay is typically set-up with horseradish peroxidase (HRP) and ABTS that culminates in the formation of a dark green compound ($ABTS^{\bullet+}$) that can be monitored at 420 nm [25]. The dioxygen consumption can also be measured in an Oxygraph® device. Finally, the stopped-flow apparatus has been widely used to find the mechanistic properties of these enzymes and it allows to follow independently the two half-reactions of the catalytic cycle by monitoring the absorbance changes at ~ 460 nm [26]. Additionally, this apparatus allows studying the kinetic mechanism and the identification of the Michaelis complex (D-glucose-Enzyme complex) of the reaction (where

disassociation occurs before the interaction of the enzyme with the final electron acceptor), compatible with a bi-bi ping pong kinetic mechanism (the typical mechanism of oxidoreductases) [26].

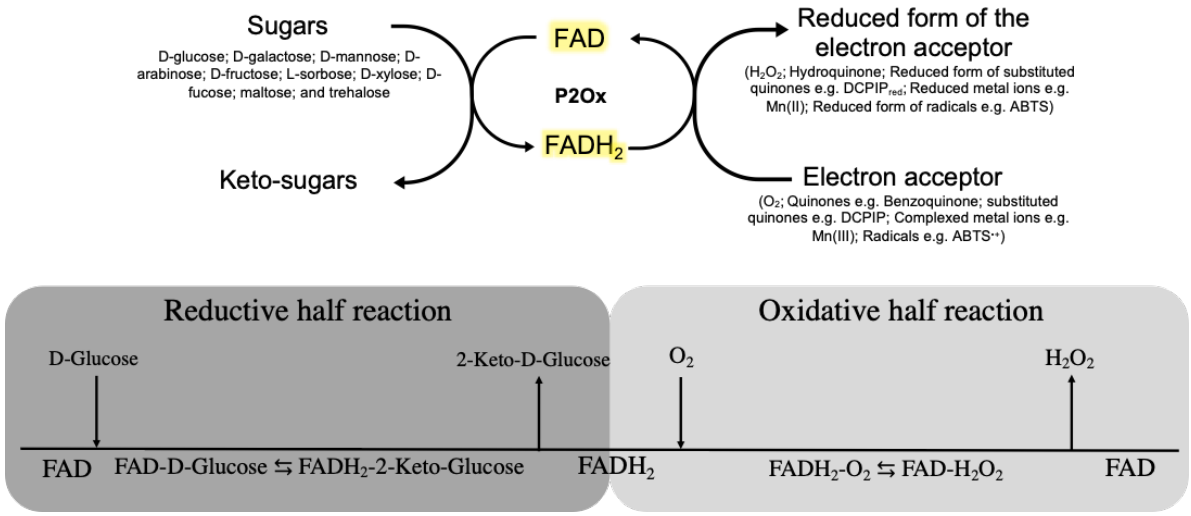

Figure 1.2. Overall redox reaction of Pyranoses 2-oxidases. On the top it is displayed the general catalytic cycle of P2Oxs that can use several sugars as electron donors releasing the correspondent keto-sugars. In the presence of electron acceptors such O_2, quinones, substituted quinones, complexed metal ions or radicals, the $FADH_2$ transfer the electrons releasing the reduced form of the electron acceptor and regenerating the FAD cofactor. On the bottom it is shown the Cleland notation of the proposed bi-bi ping pong mechanism of P2Ox whereas it is possible to divide the overall reaction into two half-reactions. During the reductive half-reaction, the FAD is reduced, and the oxidized sugar is release before the starting of the oxidative half-reaction in which the enzyme cofactor is re-oxidized regenerating the cofactor for a new enzyme turnover.

1.4 Fungal Pyranoses 2-oxidases

P2Oxs were originally studied from Fungi and the first enzyme was isolated from the basidiomycete fungi *Polyporus obtusus* in 1975 [27]. Currently, ten fungal P2Oxs mainly from white and brown-rot wood degrading basidiomycetes have been investigated [4], [28]. The fungal enzymes are homotetrameric, many times glycosylated, and the FAD co-factor is typically covalently linked to the apoprotein by a histidyl linkage [4]. Fungal P2Ox are hypothetically expressed with an N-terminal prepropeptide which can target the enzyme to hyphal periplasmic space from where they can be secreted in later stages of the fungal life cycle to act as exoenzymes [29], [30]. Their physiological role has been associated to its oxidase activity which supplies hydrogen peroxide during the catalytic cycle that can be putatively used as co-substrate for lignin-degrading peroxidases (*e.g.* dye-decolorizing peroxidases) [31], the reason why these enzymes are classified as members of the auxiliary activity family 3 of redox enzymes by Carbohydrate Active Enzymes (CAZy) (www.cazy.orf) [32]. The hydrogen peroxide released during the redox cycle of P2Ox can also have some antifungal properties against phytopathological fungus [33]. Moreover, it has been considered that the dehydrogenase activity of these enzymes shows a relevant role in the maintenance of quinone/hydroquinone redox cycle equilibrium in decomposing wood process as well as in the regeneration of reducing metals for radical based lignin depolymerization reactions [34].

Metabolically, the C2 oxidation of D-glucose by P2Oxs releases 2-keto-D-glucose that can act as an intermediate metabolite of a secondary pathway which leads the formation of the antibiotic cortalcerone, hypothetically responsible for protection against bacterial attack and/or advantage in nutrients competition with bacteria [35], [36].

There are only three known crystal structures of P2Oxs of fungal origin: *Trametes multicolor* (synonym *Trametes ochracea*) [9], *Peniophora sp.* [37] and *Phanerochaete chrysosporium* [38]. P2Ox from *T.*

multicolor, TmP2Ox, has been the one most studied P2Ox and the association between structure and function in this protein was an important step to elucidate the mechanistic action of P2Oxs. For example, using TmP2Ox it was demonstrated that the structure of each subunit of the homotetramer has a peanut-shaped with three distinct regions. An oligomerization arm responsible for the association of the protein monomers, an head domain with a putative function associated with immobilization of the protein on the fungal cell-wall polysaccharides and a protein core domain [9]. The core domain is subdivided in a FAD-binding subdomain (F subdomain) that features a Rossmann fold motif in which FAD cofactor is covalently linked to a histidine residue (His167), part of the ^{165}STHW^{169} conserved motif [9], [15]. The substrate-binding subdomain (S subdomain), bigger than the F subdomain contains the active-site cavity, in the interior of the protein, three peripherical α-helices and a six-stranded β sheet in the central part [9].In each subunit, the sugar substrate has to cross through an internal cavity that contains water molecules before reaching the enzyme active site. The residues His548, Asn593, Gln448, His450, and Val546 showed an important role in the sugar stabilization inside the substrate pocket and the alignment of the available sequences revealed that these residues are conserved among fungal P2Ox. The histidine 548 was originally hypothesized to act as a base, allowing the deprotonation of the sugar substrate in the alcohol moiety of C2, followed by hydride transfer to the N5 atom of the FAD cofactor and the Asn593 is proposed to participate in the interaction enzyme-sugar complex by the formation of a hydrogen bond with the deprotonated C2-OH moiety [9].

Very recently, and based in TmP2Ox studies, it was proposed a new mechanism for the reductive half-reaction performed in which P2Oxs show five mechanistic steps before the complete FAD reduction (Figure 1.3) [39]. In this new study, it was proposed for the first time in flavoproteins that the oxidation of a C-H bond can occur through a hydride transfer between the C2 of the sugar to the N5 of FAD, generating a protonated ketone sugar intermediate (stabilized by the key residues Thr169, His548, Asn593, and Phe474). The reaction mechanism follows with a proton transfer from the protonated keto-sugar to a conserved His548 residue culminating in the release of 2-keto-glucose and in the reduction of the protein cofactor [39].

The activity of TmP2Ox is proposed to be controlled by a highly conserved loop (residues 452 to 461) that is determinant for substrate binding and catalysis in each subunit. In the models performed with different ligands, this loop displayed two different forms, a closed and an open conformation, depending on the stage of the P2Ox redox cycle [9]. The transition between both conformations was associated with the loop motif ^{454}FSYG^{457} that becomes closer to the active site in the oxidative half-reaction blocking the entrance of sugar substrates to the pocket but still allowing the interaction with small molecules such as dioxygen [9].

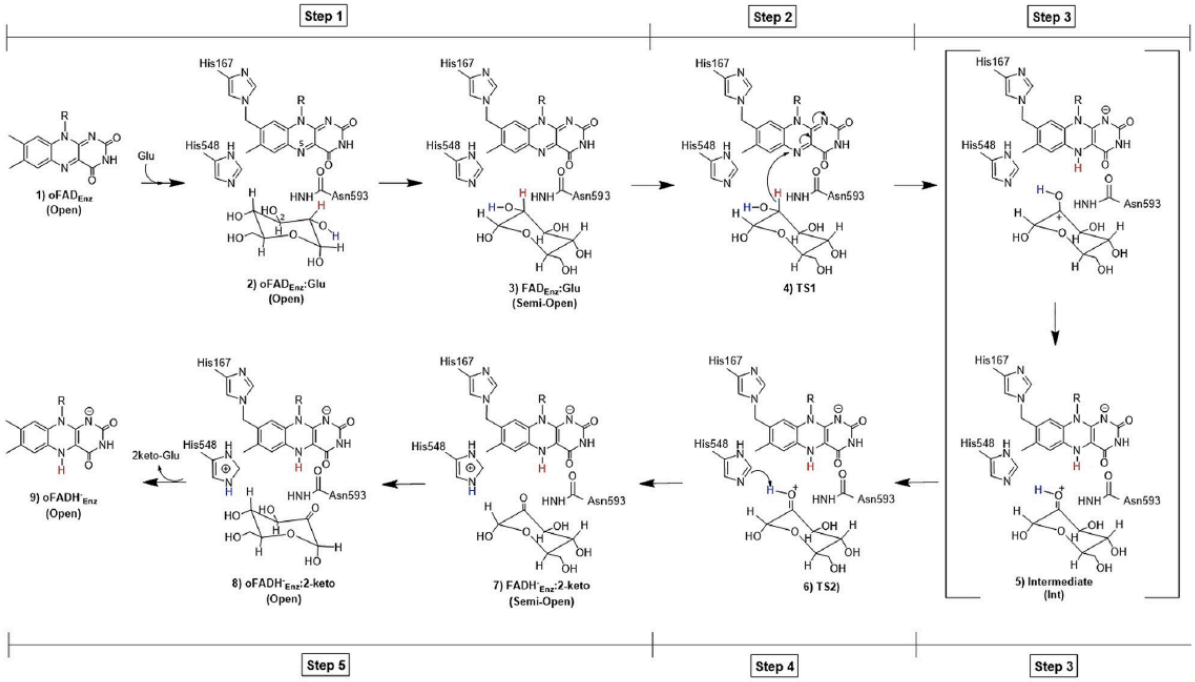

Figure 1.3. Recent proposal on the mechanistic steps of reductive half-reaction of TmP2Ox. The figure shows the steps proposed by Wongnate *et al* [39] for the reaction of P2Oxs with glucose. In Step 1 the formation of the active enzyme substrate complex (FAD_{Enz}:Glu) takes place. In step 2, the hydride transfer from the carbon position 2 of glucose to the N5 of the flavin occurs. Step 3 relates to the formation of the protonated ketone intermediate (Int), while in step 4 the proton transfer of the protonated keto to His548 takes place. In step 5, 2-keto-glucose is produced and the reduced flavin generated. Figure and descriptive subtitle taken from [39].

1.5 Bacterial Pyranoses 2-oxidases

The first bacterial P2Ox named AsP2Ox was characterized from the dry desiccation resistant actinobacteria *Arthrobacter siccitolerans* (renamed for *Pseudoarthrobacter siccitolerans* [40]) in 2016, based in sequence analysis and alignment with different GMC family members and also fungal P2Ox enzymes [24]. The AsP2Ox show highly conserved residues in the GMC family (13 out of 15 residues) and additionally, contains three major conserved regions in this family: the FAD-binding domain, the attachment loop, and the substrate-binding domain. Additionally, multiple alignment analysis with four pyranoses dehydrogenases (members of GMC family) and with three fungal P2Ox revealed an identity of 26 %, around the double obtained in the comparison with pyranoses dehydrogenases suggesting that AsP2Ox is more related with fungal P2Ox than with other members of GMC enzyme family [24].
Within the AsP2Ox sequence, the flavin binding domain was shown to be conserved when compared with fungal P2Oxs but the STHW motif that would allow the covalent ligation of FAD to apoprotein have a replacement of serine and threonine for two alanines (AAHW). These aminoacidic changes can putatively interfere in FAD ligation leading to a non-covalently bond to the apoprotein with consequences in protein stability and lower redox potential [12], [24]. Besides, the tertiary structure model suggests that in AsP2Ox His440 and Asn484 are conserved and putatively exert the same role as His548 and Asn593 of TmP2Ox.
The characterization of the recombinant enzyme shows that the optimal temperature of AsP2Ox is 37ºC. The optimal pH activity and also the kinetic parameters were re-evaluated in this thesis and will be discussed in the Results and Discussion section. The role of the AsP2Ox in *A. siccitolerans* is not well understood but the high K_m values for D-Glucose (see below) of this enzyme suggests this is not the intracellular substrate, although within the sugar substrates tested it is still the preferred one.

Two more P2Oxs from bacterial origin were later identified from soil and environmental bacteria. PaP2Ox, is from *Pantoea ananatis*, a γ-proteobacteria with a cosmopolite distribution that acts as endophytic lignocellulolytic bacterium [41], while KaP2Ox is from *Kitasatospora aureofaciens* (formerly *Streptomyces aureofaciens*) that belong to actinobacteria and is a microorganism that in its genome contains genes that codifies for lignocellulosic enzymes which suggest with a role in plant biomass degradation [28].

The PaP2Ox enzyme shares a sequence similarity of 27 % with TmP2Ox and 26 % with AsP2Ox. This protein shows two conserved domains: a FAD-binding domain, and a steroid-binding domain with unknown function but that can hypothetically act as a substrate-binding domain. Like the fungal counterparts, PaP2Ox is an homotetramer where the FAD-binding domain does not exhibit the characteristic fungal motif STHW mentioned before resulting in a FAD non-covalently bonded to each subunit, although this protein has an optimal temperature of 50ºC which is higher than the one obtained for AsP2Ox but still less thermostable as compared with fungal P2Oxs [41]. PaP2Ox showed that in conjunction with bacterial laccases can originate diverse compounds from lignin which makes it an interesting enzyme for biotechnological applications [41].

KaP2Ox, the most recently identified bacterial P2Ox showed an identity of 39 % with TmP2Ox matching 545 out of 623 of its residues. The structure in solution of KaP2Ox, unlike the previous P2Ox, is a homodimer, and the FAD is covalently bounded to apoprotein. The sequence of KaP2Ox show one Histidine (His464) that can be homologous to His548 in TmP2Ox [28].

A phylogenetic analysis based on sequences maximum of likelihood grouped KaP2Ox with other putative bacterial P2Ox in one clade distinct from fungal P2Ox but interestingly AsP2Ox was placed in another different clade far from PaP2Ox and KaP2Ox [28].

1.6 Other biotechnological applications of P2Oxs

In the late nineteenth century and early twentieth century, significant advances were made in the extraction, characterization and commercial exploitation of enzymes [42].

The potential of P2Ox in C2 regioselectivity oxidation is very promissory for the carbohydrate chemistry industry allowing the development of efficient ways to convert bulk carbohydrates in valued products [43]. Using D-glucose as substrate, P2Ox can provide 2-keto-D-glucose which can act as intermediate of other sugar precursors for the production of rare sugars, fine chemicals, and drugs [22]. For example, the antibiotic cortalcerone can be produced synthetically from the 2-keto-D-glucose supplied by P2Ox activity followed by dehydration using another enzyme [44], [45].

In the same field, an engineered P2Ox was recently used to perform the first reaction of a cascade in the one-pot bioconversion of L-arabinose to L-ribulose leading to higher production yields and replacing a process that resulted in almost 90 % of substrate waste [46]. In this cascade, the fungal P2Ox is responsible to convert L-arabinose in 2-keto-arabinose that is further converted in L-ribulose by a xylose reductase. Interestingly the conversion of L-arabinose to L-ribulose represents an increasing value from 0.1 US$ g^{-1} to 995 US$ g^{-1} which makes the investment on this enzyme as catalyst rewarding [46]. It was reported that P2Ox can also produce 2-keto-D-galactose a precursor for the production of the rare, low-caloric and noncariogenic sugar D-tagatose [43], [47] or 2-deoxy-3-keto-D-glucose that can be an intermediate for vitamin B1 and B6 production [43].

Lastly, the oxidase activity of P2Oxs can be employed as a dioxygen scavenger providing anoxic conditions that are usually hard to achieve in analytical chemistry procedures [48]. P2Ox was used in an oxygen removal system in a small open volume of a biofuel cell and the results suggested that these enzymes can be applied without interference on the biosensor detection characteristics neither in the pH

of solution which represent an advantage comparing for example, with GOx that requires a strong ionic strength buffer to maintain the pH [48].
Fungal P2Ox had been engineered for improved characteristics such as the reactivity for O_2 [49], increased thermostability [50], pH stability [50], substrate specificity and/or catalytic efficiency [46], [51], [52]. These improvements were performed using all the three methods of protein engineering (rational, semi-rational or directed evolution) with different final purposes (such as for biofuel cells [49] or biocatalysts for industry [46]).

1.7 Protein engineer: How to make better enzymes?

Enzymes are biomolecules that occur in nature associated with living organisms but they can also be synthesized *de novo* mimicking native enzymes [53]. Nowadays the *de novo* synthesis approach starts to have some impact because of the challenging of engineer native enzymes although the bulk of enzymes are still discovered and characterized from nature [53].
The major problem with organisms' native enzymes is that they are synthesized intracellularly with a defined metabolically role at relatively low levels, in amounts that are not cost-effective for commercial and industrial applications. Moreover, in most cases they show poor stability, low activity for alternative substrates, (product) inhibition and limited conversion yields [54].
Protein engineer is a revolutionary branch of science that works with different techniques to allow improving enzymes properties within short time frames [55].
Typically, protein engineering uses recombinant proteins that are usually expressed in *E. coli* systems and amino acid substitutions can be accessed by two main approaches rational design and directed evolution that can be applied individually or in conjugation to achieve the best-improved variant hits [56]. In some cases, another method a semi-rational design approaches that shares characteristics of both can also be applied.

1.7.1 Rational design in protein improvement

When an enzyme has the structural and biochemical data available and the relationship between structure and function is relatively well known, the rational design can be considered a good approach to improve enzymes [57]. This method relies on computational and biochemical studies that allow identifying residues that if mutated for others can increase the fitness of the enzyme. The methods to introduce mutations in a gene (pre-cloned onto an expression vector) in rational design is based in site-directed mutagenesis (SDM) which use a pair of designed oligonucleotides primers carrying a nucleotide that will mismatch with the template sequence allowing the change of nucleotide sequence after a PCR reaction with an high-fidelity DNA polymerase [58]. There are more than one strategy to design primers for SDM (the mutation can be in both primers or in only one primer and the other will pair fully with template, for example) but all of them results in a linear PCR product, that is digested (*e.g.* with DpnI) to eliminate template sequences, and then used to transform *E. coli* strains. In these bacteria self-mechanisms, turn the PCR product, in a circular plasmid that allow for expression of the gene of interest [58].
In this technique, the correct introduction of the mutations is confirmed by DNA sequencing followed by enzyme production, purification and biochemical characterization [59], [60] (Figure 1.4). If the variant is not as good as expected, all computational analysis could be performed again, and the experimental procedure has to be repeated. Due to the fact of this approach relies on specific operator-defined mutations it is a good technique to test a pre-elaborated hypothesis on the structural and mechanistic role of specific residues [58].

1.7.2 Directed evolution: using Darwinian evolution principles to improve biocatalysts

When the crystal structure or the model structure of an enzyme is not available the application of rational design does not apply. If an enzyme has N amino acids and considering 20 amino acid possibilities for each position, there is a space of possible enzyme variants given by 20^N [61]. This imaginary space of hypothetically mutant enzymes hides variants with so far undetected characteristics although the time limitations just allow us to explore a tiny part of them.
The directed evolution (DE) technique, also known as laboratory evolution, appears in the 1980's to bypass that gap [60].
In DE, the concept is to simulate *in vitro,* speeded-up, evolutionary trends that occurs in nature which leads organisms with improved fitness when compared with ancestors. The well-adapted enzyme mutants, during protein engineer through DE, are selected as parent for further rounds to improve some characteristic(s), this process is repeated iteratively simulating a process that, in nature, could take hundreds or thousands of years [62].
The major advantage of DE is that mutations are introduced randomly in the protein gene without the need of previously computational analysis [60].
The usage of DE requires four main prerequisites as follows, (I) the availability of the gene that codifies for the protein that will be engineered, (II) a suitable expression system, (III) a method to generate diversity onto parent gene (library) and (IV) a method to screen and select the improved variants within the library [63]. For the first and second pre-requisites, the most common approach is to have a gene of the desired protein cloned into a plasmid vector that could be heterologously expressed in *E. coli* cells.

1.7.2.1 Generation of diversity on the parent gene

The creation of diversity on a gene can be performed using two main distinct techniques: random mutagenesis or recombination [60], [64], [65].
In random mutagenesis the introduction of mutations to construct a variant library can be performed using, for example, chemical and/or physical mutagenesis, mutator strains, but the most used approach is the error-prone PCR (epPCR) (Figure 1.4) [64].
In epPCR the gene that codifies for the protein of interest is amplified in low fidelity conditions using a polymerase that usually can introduce mutation mistakes during elongation of DNA strand (*e.g.* Taq polymerase). Additionally, several factors can be optimized to tune mutation rates, increasing the concentration of $MgCl_2$, use of mutagenic dNTPs analogs, increase the DNA polymerase concentration, increase the number of cycles or inclusion in the PCR mix compounds that interfere in Taq polymerase elongation (*e.g.* $MnCl_2$) [66], [67]. These conditions should be optimized to achieve a relatively low mutation rate (2-3 mutations in a gene) which amplify the probability to achieve beneficial mutations and prevent the introduction of exceeding mutation numbers that culminate in non-functional proteins [60]. During the PCR the Taq polymerase has a high tendency to replace A to G and T to C which can lead to a higher GC content of product sequence and also limited diversity of mutations achieved. Sometimes to counteract this tendency the concentration of dNTPs used in the PCR mix can be unbalanced [66].
Gene recombination is also used to create enzyme gene variants randomly. The most common recombination technique is named DNA shuffling. In this approach, chimera enzymes that result from the association of diverse homologous genes are constructed [64]. The genes used in DNA shuffling

could derive from variants of the same protein or from genes from different origins that codify for structurally similar protein, showing high homology [54], [68]. A common protocol of DNA shuffling includes a controlled fragmentation of the gene (50 to 150 bp) with DNase I and then all fragments are joined randomly in a PCR without primers because the fragments by themselves can align and cross-prime to each other [56]. Next, a standard PCR with appropriate flanking primers is performed to amplify the low number of segments that are full-length, generating a gene library with different chimeric genes. The size of a recombinant library is typically smaller than a library generated by random mutagenesis [56], [60], [69]. However, the great advantage of DNA shuffling is that in later stages of random mutagenesis evolution it can be applied to accumulate the beneficial mutations and eliminate the deleterious or neutral mutations [70].

1.7.2.2 Screening and selection in directed evolution

Finally, in DE, the development of a suitable method to screen and/or select the enzyme variants of a library is mandatory and is considered the most challenging step [64].
Screening methodologies are developed in order to discover phenotypes associated genotypes and to allow to identify improved enzyme variants for the desired characteristic [64]. The screening methods are wide diverse, but they can be grouped into three major types that englobes screenings of spatially separated variants, high-throughput screenings in flow cytometry and screening in artificial cell-like compartments [64].
In spatially separated variant screenings the library size is small (~10^4 variant members per screening round) [64]. The main advantage of this approach is its compatibility with several assay techniques, including screening in solid media by, for example, following the zones of degradation of a substrate in agar plates surrounding the colonies, or in liquid medium, that are usually performed in multi-well plates using a coupled assay by, for example, fluorescence spectrophotometry (Figure 1.4). Both solid and liquid media screenings are typically based in single *E. coli* colonies that contain one gene variant and the respectively expressed variant enzyme. The main disadvantage of these screenings is the high time-consumption which limits the throughput capacity [64], [65].
Flow cytometry screenings are performed in a fluorescence-activated cell sorting (FACS) apparatus and the size of the library can be higher than in the methods described before (> 10^8 members can be analyzed in less than 24 h) [65]. In this approach, the aim is to analyze individually each cell that could emit fluorescence (or luminescence), for example, by monitoring the level of expression of reporter proteins such as green fluorescent protein (GFP) that were coupled to the target enzymes [71]. The FACS stringency can be adjusted which allows to perform different rounds with an increment of this parameter using the gate of cell sorted in the round before. Cell surface display can as well be performed with the help of FACS to sort positive improved mutants. In this approach, the aim is to develop a system that allow the display of the target protein in cell surface (for example via anchoring) followed by treatment with modified antibody's (coupled with fluorophores) that will allow identifying the desired enzyme variants [64], [65].
The screening in artificial cell-like compartments are used in cases of hard establishment of a cell system that allow the implementation of a fluorescent reporter for a given gene and phenotype [65]. Then, *in vitro* compartmentalization (IVC) can provide an alternative method to high throughput using the FACS apparatus. The main advantage of this system is the inexistence of the diverse metabolic network of the cells eliminating the possibility that improved phenotypes come from mutations non-related with target gene [64], [65]. In IVC approach aqueous droplets are used in water-in-oil emulsions (or also droplets in water-in-oil-in-water emulsions) to compartmentalize individual genes and gene products with alternative fluorogenic substrates.

As an alternative to the screening methods that require the individual evaluation of phenotypes, selection methods link the desired activity to a physical separation of the encoding DNA or survival of the organism producing active library members [65]. "Rejective to the unwanted" is the feature of selection methods that make them pure high throughput [65]. DE selection methods include several techniques such as cell surface display and cell compartmentalization that are very elaborated techniques with several variations [65]. Other technique that is used for selection in DE of enzymes with active role in cell metabolism is organismal growth complementation (or organismal survival) in which the desired enzyme property is coupled with the fitness of the host cell allowing that only the cells containing the protein with the desired property can survive under selective pressure [65].

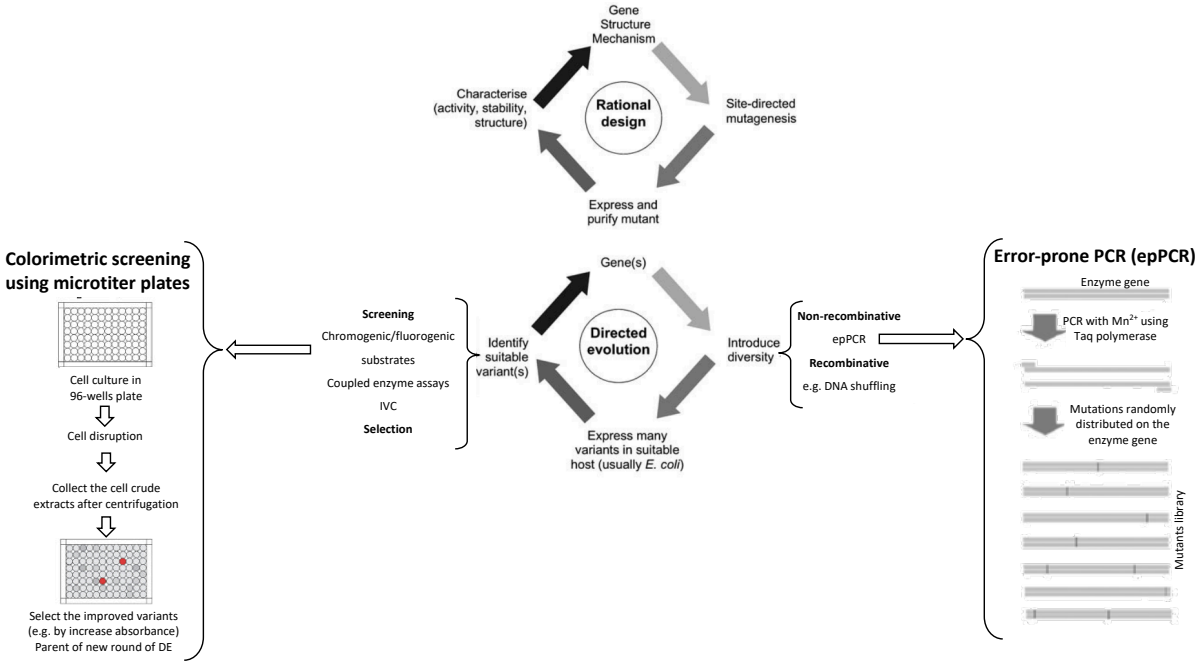

Figure 1.4. Comparison of the main steps of rational design and direction evolution. In the scheme four main steps are displayed related with protein engineering by rational design or directed evolution. Within directed evolution, the main procedures are exemplified, how epPCR is performed and also exemplified is a high through put screening using microtiters and a chromogenic assay that allow to identify the best hit variant to be used as parent of a new round of directed evolution. The directed evolution technique is iterative, *i.e.* when a new parent is achieved all steps (generation of diversity, expressing in host system and screenings) are repeated. The figure was adapted from [60].

1.7.3 Semi-rational design in protein engineering

The semi-rational design approach for enzyme engineering uses the site-saturation mutagenesis (SSM) technique. This method is a conjugation between rational and non-rational. In a first step, computational analysis based on protein structure, identify amino acids that could interfere directly on the improvement of the desired property. In a second step, the replacement of that amino acid position will be performed for the other nineteen amino acids available, creating a small library of enzymes (called smart library) that will be screened for activity (as a DE library) [68].

In SSM the mutations are introduced by mutagenic primers that are synthetic oligonucleotides with randomized codon flanked by parent sequence. These primers are degenerated, and their sequence is identical with the parent template except in the specific position where the mutation will be introduced by the randomized codons. After a standard PCR reaction with mutagenic primers, the library is constructed [54]. This approach can be applied to randomize several positions simultaneously creating a library with variants for more than one position [54].

1.7.4 The New Era in protein engineering: bioinformatic and machine-learning approaches

Computational protein design is an *in silico* technique that relies on semi-rational design [56]. In computational protein design, the aim is to apply a combination of force field and algorithms to provide different tridimensional configurations of the same protein in which all amino acids can be substituted by other nineteen resulting in proteins with different energies. The ones with lower energy are chosen to test experimentally [56].
Machine-learning-guided directed evolution for protein engineer is a new tool that is nowadays being an intensive target of research. The concept is to create DE principles in computing-based programs without the need for experimental screens and selection. This approach allows to bypass the time-consuming and expensive DE approach and also to overcome problems related with constrains in evolution imposed in DE [72]. However, it is still not possible to predict how much time can be saved using this process. Instead of DE that uses only the improved variants, in machine-learning-guide processes, information of unimproved sequences are used to expedite evolution and expand the number of properties that can be optimized [72]. The most challenging part of this method is to build a sequence-function model that can be applied to choose sequences to screen. In the end, machine-learning-guided DE uses all information of the sequence-function pairs to construct a landscape to achieve improved sequences. [72].

1.8 Context of the project

In this master thesis the aim was to apply directed evolution methodologies, one of the main focus of Microbial and Enzyme Technology Lab at ITQB, to identify improved variants of AsP2Ox, a bacterial pyranose 2-oxidase recently characterized in this laboratory.
The goal was to achieve variants exhibiting higher catalytic efficiency and lower K_m for D-Glucose and O_2 allowing its application as first generation biosensors for monitoring the D-glucose levels replacing the typical GOx or GDHs.
When I arrived at the Microbial and Enzyme technology (ITQB), the directed evolution of AsP2Ox was already being performed by a fellowship researcher. After a round of DE and rational design a variant, CM3, had been identified, showing a catalytic efficiency for D-glucose and O_2 around 10-fold higher than the wild-type. When I started the studies two initial tasks were planned based on identified issues. The first concerned the cell cultivation at large scale (5L-Erlenmeyers containing 1L of LB medium) where a lack reproducibility was identified; many times, cell cultures die before the induction of gene expression with IPTG. This led me to investigate alternative *E. coli* strains. The second, related to literature that reported that the oxidized form of ABTS ($ABTS^{\bullet+}$), produced upon activity of HRP, in the coupled assay to measure AsP2Oxs activity, could act as an electron acceptor of AsP2Ox, competing with O_2 and resulting in non-reliable activity measurement. This aspect needed investigation since if this is confirmed all previously optimized DE procedures need re-validation and re-optimization as well as the characterization of wild-type, intermediates and hit variant.

The work performed resulted in the optimization of the cultivation at large-scale of recombinant *E.coli* strains producing AsP2Ox, optimization of the coupled enzymatic assay to measure activity of wild-type and AsP2Ox variants, re-investigation of kinetic parameters and successful implementation of a DE protocol to improve the first P2Ox from bacterial origin, in which the diversity of the gene was promoted by epPCR and the screening method was implemented based on a reaction coupled assay with

HRP monitored by UV-Vis absorbance. Hit variants were identified and the proteins were purified and biochemically characterized showing improved remarkable kinetic properties.

2. Material and methods

2.1 General materials and procedures

2.1.1 Bacterial strains, plasmids and cultivation medium

During this study the Tuner (DE3, Novagen), KRX (Promega), Rosetta (DE3, Novagen) and BL21 star (DE3, Novagen) *E. coli* strains were used to heterologously express the different AsP2Ox variant genes previously cloned onto pET-15b vector (Novagen). In BL21 star, Tuner and Rosetta the target genes are controlled by T7 promoter, induced by isopropyl β-D-1-thiogalactopyranoside (IPTG) and in the KRX strain the genes are under control of rhaPBAD promoter, induced by rhamnose. The pET-15b vector has some important characteristics, namely a region that codifies for a β-lactamase that confers the resistance to ampicillin and a region that codifies for a 6xHis tail localized close to the cloning site that allow the protein produced to be purified using an His-tag affinity column. Luria-Bertani (LB) and Terrific Broth media (TB) were used as routine liquid media to grow the different *E. coli* strains. The cultivation media was supplemented with 100 μg/mL of ampicillin (NZYTech) for all strains that were transformed with the plasmid pET-15b carrying the *asp2ox* gene plus 20 μg/mL of chloramphenicol (NZYTech) when the host strain used was Rosetta. LB medium contains (*per* liter): 1 % of tryptone, 0.5 % of yeast extract and 170 mM of NaCl. TB medium contains the following components (*per* liter): 1.2 % of tryptone, 2.4 % of yeast extract, 4 mL of glycerol (86%), 17 mM of KH_2PO_4 and 72 mM of K_2HPO_4. Super Optimal Growth medium (SOB) was used for the culture of electrocompetent cells. SOB medium contains (*per* liter): 2 % of tryptone, 0.5 % of yeast extract, 10 mM of NaCl and 2.5 mM of KCl, 10 mM of $MgCl_2$ and 10 mM $MgSO_4$. Luria-Bertani Agar (LA) was used as the solid media and has the same composition than LB with addition of 1.5 % of bacteriological agar. All culture media was sterilized in an autoclave at 121ºC and stored at room temperature until use.

2.1.2 Preparation of electrocompetent *E. coli* cells

The frozen stock of *E. coli* strains from the Lab culture collection was used to stretch a LA plate that was incubated overnight at 37ºC. In the following day, one single colony was picked to inoculate 20 mL of SOB medium (pre-inocula) and the cultures had grown overnight at 37ºC, 180 rpm on Innova 44 incubator shaker (New Brunswick Scientific. This incubator was used for all growths except when 96-wells plates were used). Growth in 250 mL of pre-warmed SOB medium started with $OD_{600nm} \simeq 0.01$ using the pre-inocula. Culture were incubated at 37ºC, 180 rpm. After 3 h ($OD_{600nm} \simeq 0.8$), the Erlenmeyers containing the cultures were placed in an ice-cold bath for 20 min (after this step all procedures were performed at 4ºC). Cultures were transferred to ice-cold centrifuge bottles and spun down (4420 × g, 10 min at 4ºC). The supernatants were discarded, and the cell pellets were washed with 250 mL of a sterile ice-cold 10% glycerol solution. The cells were centrifuged again in the same conditions. The washing step was performed twice. The final cell pellets were resuspended in 10 % glycerol solution that remained in the centrifuge bottles. Aliquots of 150 μL were frozen at - 80ºC and stored until use.

2.1.3 Transformation of *E. coli* cells

One microliter of purified plasmid (~150 ng of DNA) was added to an aliquot of 150 µL electrocompetent cells previously thawed on ice (for approximately 10 min). This mixture was transferred to a sterile and ice-cold electroporation *cuvette* (0.2 cm gap), which was placed in the Xcell ShockPod chamber (Gene Pulser XcellTM, Biorad) and pulsed using set conditions of C = 25 µF, PC = 200 Ω, V = 2.5 kV. Immediately after the pulse, 1 mL of SOB medium was added; the cell suspension was transferred to an Eppendorf and incubated at 37ºC for 1 h, 180 rpm. The transformed cell aliquots were diluted (to obtain single colonies) and the dilutions were spread to an LB agar plate supplemented with the appropriate(s) antibiotic(s) and incubated at 37ºC overnight.

2.2 AsP2Ox large-scale production and purification

2.2.1 Optimization of large-scale production

To select the best expression strain for large-scale production (2.5 L) three *E. coli* strains were tested in small-scale production (50 mL): BL21 Star, Tuner and Rosetta. Each strain was transformed (as described in section 2.1.3) with the pET-15b carrying the wild-type *asp2ox* gene. The cells from the transformation were plated on LA plates pre-supplemented with 100 µg/mL of ampicillin (and additionally with 20 µg/mL of chloramphenicol for Rosetta strain). The plates were incubated overnight at 37ºC.

In the following day a pre-inocula were performed by picking a single colony from the LA plates to a 250 mL Erlenmeyer containing 50 mL of LB supplemented with antibiotics mentioned. The cultures had grown for 17 h at 37ºC, 180 rpm.

In the following day, 50 mL growths at an initial $OD_{600\ nm} \approx 0.05$ were performed in duplicate for each strain. Growths proceed at 37 ºC, 180 rpm. The increase of optic density at 600 nm was monitored using Nicolet Evolution 300 spectrophotometer (Thermo Industries, Waltham). When $OD_{600\ nm}$ reached 0.8 A.U. one of the duplicates for each strain was induced with IPTG at a final concentration of 100 µM. After this, the temperature was decreased to 25ºC and all cultures grew overnight at 180 rpm. The cells were collected by centrifugation (4420 × g, 10 min at 4ºC). The cell pellets from the growths were disrupted using a French press (Thermo IEC) operating at 900 psi in a process repeated 5 times and the lysed suspension was centrifuged to remove cell debris (39200 × g, 2 h at 4ºC). The supernatants (crude extracts) were collected. For SDS-Page analysis, each well of the gel was loaded with ~ 20 µg of protein (quantification by Bradford method) of each crude extract.

2.2.2 Optimized large-scale production and purification of recombinant AsP2Ox variants

For the production of AsP2Ox enzyme variants at a larger scale *E. coli* Rosetta strain was used. The transformation of *E. coli* Rosetta with the plasmid carrying the different AsP2Ox variants was performed as described in section 2.1.3. Single colonies in LA plates were used to inoculate 50 mL of LB medium supplemented with 100 µg/mL ampicillin and 20 µg/mL chloramphenicol and, the cultures grew overnight at 37ºC, 180 rpm. In the following day, the pre-inocula were used to inoculate 2.5 L of LB medium supplemented with 100 µg/mL ampicillin and 20 µg/mL chloramphenicol in a Corning® 5L Baffled PETG Erlenmeyer flask. The initial OD_{600nm} was approximately 0.1. Cultures were incubated at 37ºC, 100 rpm and when OD_{600nm} reached 0.8, 100 µM IPTG was added and the growth continued at

25ºC, 100 rpm in the same incubator. After approximately 17 h of growth, cells were collected by centrifugation (4420 × g, 15 min at 4ºC) and stored in aliquots at -20ºC.
For purification, the cell pellets were unfrozen and resuspended in a 3-10 mL of 20 mM Tris-HCl buffer, pH 7.6. The final cell suspension was supplemented (*per* mL) with 2 µL of proteases inhibitor mixture (1.75 mM antipain and 2.5 mM leupeptin), 1 µL of 1 U/mL DNAse I and 5 µL of 1M $MgCl_2$. The disruption of cells was carried out in a French press (Thermo IEC) operating at 1000 psi in a process repeated 5 times, allowing the maximal cellular rupture. Cell debris was removed by centrifugation (39200 × g, 2 h at 4ºC). The protein purification was performed in an ÄKTA purifier system (GE Healthcare). The crude extract was loaded onto a 1 mL- or 5 mL-HisTrap HP column (GE Healthcare) pre-equilibrated with 20 mM Tris-HCl buffer, pH 7.6 (supplemented with 0.2 M NaCl and 10 mM imidazole). Elution of the AsP2Ox protein from the column was performed by applying a 0-100 % gradient of 1 M imidazole in 20 min with a flow rate of 1 mL/min. The yellow protein fractions were collected, pooled and applied in a PD-10 desalting column (GE Healthcare) in order to change the buffer for 20 mM Tris-HCl buffer, pH 7.6 with 0.2 M NaCl (without imidazole). Glycerol was added to the enzyme preparations to a final concentration of 20 % and the aliquots were stored at -20ºC. SDS-gel analysis was performed to check the purity of protein preparations. Additionally, the quality of the purified protein was evaluated by checking the characteristic bands of FAD absorption at 390 nm and 460 nm in UV-Visible spectra (data obtained in Nicolet Evolution 300 spectrophotometer from Thermo Industries - Waltham).

2.2.3 Determination of protein concentration

Total protein concentration was determined using the Bradford assay or Abs at 280 nm (ε_{280}= 65440 M^{-1} cm^{-1}, value obtained considering the amino acidic composition of the protein and also the contribution of the FAD). The ratio of FAD *per* protein molecule is 1:1 then the protein preparation is fully FAD loaded. In order to assess FAD depletion and calculate the active fraction of enzyme preparations, the FAD content of enzyme preparations was quantified by measuring the absorption of protein at 450 nm in Nicolet Evolution 300 spectrophotometer (Thermo Industries, Waltham). The molarity of FAD in protein preparations was determined by using ε_{450}=11300 M^{-1} cm^{-1} [11]. For all analytical procedures such as steady-state kinetics the amount of protein used was the value determined by $Abs_{450\ nm}$.

2.3 Wild-type AsP2Ox steady-state characterization using an HRP coupling assay

2.3.1 Selection of the suitable substrate system for HRP coupling assay

In order to select a reliable method to quantify the AsP2Ox activity for D-glucose and O_2, it was used a coupled assay with horseradish peroxidase (HRP). In this coupling assay, the HRP uses the hydrogen peroxide produced by AsP2Ox and its own substrates that can be oxidized originating chromogenic species. The two reduced substrates are ABTS that generates $ABTS^{\bullet+}$ (green chromogen) upon oxidation by HRP or AAP plus DCHBS that generates a pink chromogen upon oxidation with HRP.
Two preliminary tests were performed to verify if the final oxidized form (chromogenic compound) originated by HRP activity can act as electron acceptor of AsP2Ox redox cycle, which can culminate in chromogen bleaching and resulting in non-reliable measurements.

2.3.1.1 Preliminary assays with $ABTS^{\bullet+}$

$ABTS^{\bullet+}$ was generated by oxidation of 10 mM ABTS solution with CotA laccase (Martins *et al*, 2002). The solution color changed from colorless to dark green which indicates the formation of the radical cation ABTS ($ABTS^{\bullet+}$). CotA laccase was removed by ultrafiltration using an Amicon® ultra centrifugal filters (Merck) at 4000 rpm 30 min on Eppendorf 5810 R centrifuge. Spectrophotometric assays were performed in 1 mL containing 1 M of D-glucose, 80 µM of $ABTS^{\bullet+}$ and 60 µg of wild-type AsP2Ox (control assays were performed without D-glucose and with varied concentrations of AsP2Ox). The changes of absorbance at 420 nm were followed in a Nicolet Evolution 300 spectrophotometer (Thermo Industries, Waltham). All assays were performed at 37ºC in aerobic and anaerobic conditions. For the assays in aerobiosis, reaction mixtures without AsP2Ox protein were bubbled with pure O_2 during 15 min. For anaerobiosis assays, a *cuvette* with a rubber cap was used and N_2 was bubbled with a needle directly into the reaction mixture (without AsP2Ox) for 15 min. Reactions started with the addition of the wild-type AsP2Ox.

2.3.1.2 Preliminary assays using the Pink chromogen

The compound *N*-(4-antipyryl)-3-chloro-5-sulfonate-*p*-benzoquinone-monoimine, mentioned as pink chromogen in this thesis was generated mixing 0.1 mM of 4-Aminophenazone (AAP), 1 mM of 3,5-Dichloro-2-hydroxybenzene-sulfonic acid (DCHBS), 8 U HRP and 0.1 mM H_2O_2. The change of the solution color from colorless to dark pink suggest the successful production of the pink compound. HRP was removed by ultrafiltration using an Amicon® ultra centrifugal filters (Merck), at 4000 rpm during 30 min on an Eppendorf 5810 R centrifuge. Spectrophotometric assays were performed in 1 mL containing 1 M of D-glucose, 35 µM of pink chromogen, 60 µg of wild-type AsP2Ox (control assays were performed without D-glucose and with varied amounts of AsP2Ox). The changes of absorbance at 515 nm were followed in a Nicolet Evolution 300 spectrophotometer (Thermo Industries, Waltham).
All assays were performed at 37ºC in aerobic and anaerobic conditions. For the assays in aerobiosis, reaction mixtures without AsP2Ox protein were bubbled with pure O_2 during 15 min. For anaerobiosis assays, a *cuvette* with a rubber cap was used and N_2 was bubbled with a needle directly into the reaction mixture (without AsP2Ox) for 15 min. Reactions started with the addition of the wild-type AsP2Ox.

2.3.2 pH profile of AsP2Ox wild-type

The pH profile of wild-type AsP2Ox (as well as for all variants) was determined by the HRP-AAP/DCHBS coupling assay following the increasing of absorbance at 515 nm. All assays were performed in 200 µL volume at 37ºC. A 3 M stock solution of D-glucose was prepared in Milli-Q water and the reaction mixture contained 0.1 mM of AAP, 1 mM of DCHBS, 8 U of HRP and 300 mM of D-glucose. The routine buffer to determine the pH profile was Britton-Robinson buffer (100 mM phosphoric acid, 100 mM boric acid and 100 mM acetic acid mixed with 1 M NaOH to the desired pH). The range of pH used varied between 5 and 9. To be sure about the pH of the reaction mixture after all components were mixed, the pH in each well was measured using a pH meter BasiC 20 (Crison). The reaction started with the addition of a pre-determined concentration of purified Asp2Ox variant to each well.

2.3.3 Steady-state characterization of Wild-type AsP2Ox for different substrates using HRP-AAP/DCHBS coupling assay

Enzymatic activity of purified wild-type AsP2Ox enzyme was monitored using a Synergy2 microplate reader (BioTek) following the formation of *N*-(4-antipyryl)-3-chloro-5-sulfonate-*p*-benzoquinone-monoimine at 515 nm (ε_{515}= 26000 M^{-1} cm^{-1} [73]). All enzymatic assays were performed using at least three independent assays in triplicate. The reaction mixtures of the coupling assays to measure AsP2Ox activity contained 0.1 mM AAP, 1 mM DCHBS, 8 U HRP and different concentrations (0 – 2.5 M) of sugars (D-galactose, D-glucose, D-ribose, D-xylose or L-arabinose). The reaction buffer was 100 mM sodium phosphate buffer, pH 7.5. The buffer and the sugar's stock solutions were saturated with O_2 by bubbling pure oxygen for ~20 min. The reaction was started with the addition of enzyme. All steady-state kinetics measurements were performed at 37ºC.
Apparent steady-state kinetic parameters (k_{cat} and K_m) were determined by fitting data directly into the Michaelis-Menten equation (Origin-Lab software).
For variants 2C9* and CM3 the steady-state kinetics performed were similar than those referred above but the sugar substrate used was only the D-glucose.

2.4 Directed evolution of AsP2Ox

2.4.1 Optimization of directed evolution using 96-wells plate high throughput screening

In order to achieve the combination of conditions that confers the lowest coefficients of variation (CV) for 96-wells plate screenings (microtiter and deep-wells, with different culture media and volumes) two different *E. coli* strains (KRX and BL21 star) were tested as well as 4 methods of disruption: addition of Lysozyme (AppliChem), addition of B-PER detergent (ThermoScientific), cycles of freeze with N_2 and thaw, cycles of freeze at -80ºC and thaw.

2.4.1.1 *E. coli* growth in 96-wells plates

The transformation of *E. coli* electrocompetent cells (KXR or BL21 star) was performed with 2 µL of CM3 AsP2Ox variant plasmid (~200 ng of DNA) in the conditions described in section 2.1.3. Dilutions were performed in order to have single colonies on the LA plates previously supplemented with 100 µg/mL of ampicillin. In the following day, the 96-well plates microtiters or deep-wells were prepared by filling the edge wells, to prevent media evaporation, with 200 µL or 1 mL of bi-distillated H_2O, respectively. The remaining 60 wells were filled with 200 µL (microtiters) or 400 µL (deep-wells) of LB supplemented with 100 µg/mL of ampicillin. The wells B2 and C2 were the media contamination control (without inoculation) and all other wells were inoculated by picking the single colonies from the LA plate with sterile toothpicks. For the pre-inocula, the 96-wells plates were covered with a sealing film and were incubated at 37ºC, 750 rpm in Titramax 1000 plate-shaker (Heidolph. This shaker was used for all procedures that need it with 96-well plates) for 24 h. In the following day, new sterile 96-wells plates were prepared by filling the edge with bi-distillated H_2O, as described before while the remaining 60 wells were filled with 180 µL (microtiters) or 900 µL (deep-wells) of TB supplemented with 100 µg/mL of ampicillin. Next, 20 µL (for microtiters) or 100 µL (for deep-well) of pre-inocula were transferred. The plates were covered with a sealing film and they had grown 3 h at 37ºC, 750 rpm and then were induced with 12 mM rhamnose (for KRX strain) or 0.1 mM IPTG (for BL21 star).

Afterwards, growths proceed overnight at room temperature at 750 rpm. In the following day, the plates were centrifuged at 4ºC, 4000 rpm, 30 min on an Eppendorf 5810 R centrifuge. The supernatants were discarded and the plates with the cell pellets were stored at –80ºC until use.

2.4.1.2 Optimization of disruption method in 96-well plates

The disruption using lysozyme was performed by resuspending the cell pellets with 100 µL (in microtiters) or 200 µL (in deep-wells) of 20 mM Tris-HCl buffer, pH 7.6 supplemented with 2 mg/mL of lysozyme (Applichem). In a second approach, cell pellets were submerged in liquid nitrogen and afterwards thawed at room temperature for 5 min. After 3 cycles of freeze and thaw, cell pellets were suspended in 100 µL (microtiters) or 200 µL (deep-wells) of 20 mM Tris-HCl buffer, pH 7.6. In a third approach, cell pellets were placed at -80ºC for 15 min and then thawed at 37ºC for 5 min. After 3 cycles of freeze and thaw, cell pellets were suspended in 100 µL (microtiters) or 200 µL (deep-wells) of 20 mM Tris-HCl buffer, pH 7.6. The last approach tested was a chemical disruption using 100 µL (microtiters) or 200 µL (deep-wells) of 40 % Bacterial Protein Extraction Reagent (B-PER®, Thermo Scientific) in 20 mM Tris-HCl buffer, pH 7.6. The cell pellets were resuspended in B-PER and incubated during 20 min at room temperature at 750 rpm. For all tested methods, the plates containing the suspensions after the cell disruption were centrifuged on an Eppendorf 5810 R centrifuge (4000 rpm, 30 min at 4ºC). The supernatants were collected (cell crude extracts) and used for enzymatic activity measurements. The enzymatic activity of each plate was tested using the HRP-AAP/DCHBS coupled assay by transferring 50 µL of cell crude extracts to new 96-well microtiters containing 150 µL of reaction mixture (0.1 mM AAP, 1 mM DCHBS, 8 U HRP and 1 M of D-glucose in 100 mM sodium phosphate buffer pH 7.5). The progress of reaction was followed by the increasing of absorbance at 515 nm using a Synergy2 microplate reader (BioTek).

2.4.2 Generation of libraries of mutants

Library of *asp2ox* gene variants was generated using error-prone PCR (epPCR). The primers for the PCR were carefully designed to allow the ligation of the insert (*asp2ox* gene) into the vector by the Gibson assembly methodology [74].

2.4.2.1 epPCR of *asp2ox* gene

The gene of AsP2Ox variants were amplified using the forward primer P2OxFwdGA (5' GCAGCCGGATCCTCGAGCATTATTTAGACAGTCTATTGTCTGATTCGG 3') and the reverse primer P2OxRevGA (5' TGGTGCCGCGCGGCAGCCATATGAGCGGTCACCGGTATC 3'). The underline sequence in both primers is the region that will pair with *asp2ox* gene template. The epPCR was performed in a total volume of 50 µL reaction containing 300 ng of DNA template (pET-15b carrying *asp2ox* gene variant), 1 µM of each primer (P2OxFwdGA and P2OxRevGA), 200 µM of dNTPs, 1.5 mM $MgCl_2$, Taq polymerase buffer, 50 µM $MnCl_2$ (concentration previously determined to allow a Taq polymerase mutation rate between 1 and 3 mutations in each gene) and 2.5 U of Taq polymerase (Thermo Scientific). The PCR program was carried out in a thermal cycler (MyCyclerTM thermocycler, Biorad) at the following conditions: 2 min initial denaturation at 95ºC, 30 cycles of 1 min at 95ºC, 1 min at 69ºC and 2 min at 72ºC. Finally, after those cycles, the PCR had a step of 10 min at 72ºC. Two microliters of the amplified product was checked using agarose gel (1 %) electrophoresis in

a 40 min-run under an electrical field of 100 V (The presence of a strong band at around 1600 bp shows that the PCR was successful). The PCR product was purified using Illustra GFX PCR DNA kit (GE Healthcare). The final elution step in the purification was performed using 30 µL of milli-Q water.

2.4.2.2 PCR of pET-15b vector

The PCR of the vector (pET-15b) was performed in high fidelity conditions. The amplification was performed with the primer forward pET15bFwdGA (5' ATGGCTGCCGCGCGGCAC 3') and the primer reverse pET15bRevGA (5' ATGCTCGAGGATCCGGCTG 3'). The PCR was performed in a final volume of 50 µL reaction containing 50 ng of DNA template (pET-15b), 0.5 µM of each primer (pET15bFwdGA and pET15bRevGA), 200 µM of dNTPs, 1 U of Q5 High-fidelity DNA polymerase (New England Biolabs) and Q5 reaction buffer. The PCR program was carried out in a thermal cycler in the following conditions: 30 sec initial denaturation at 98ºC, 30 cycles of 10 sec at 98ºC, 30 sec at 71ºC and 3 min at 72ºC. After those cycles, the PCR had a final step of 2 min at 72 ºC. Two microliters of the amplified product was checked using agarose gel (1 %) electrophoresis in a 40 min-run under an electrical field of 100 V (The presence of a strong band at around 6000 bp shows that the PCR was successful). The PCR product was purified using Illustra GFX PCR DNA kit (GE Healthcare). The final elution step during the purification was performed using 30 µL of milli-Q water.

2.4.2.3 Digestion of PCR products and ligation of *asp2ox* gene to vector (Gibson assembly).

To avoid the presence of the DNA template in the PCR products preparations, a digestion with DpnI was performed for both PCR products (gene and vector). The enzyme DpnI cleave the restriction site when the DNA strains are methylated (bacterial pattern). The digestion was carried in 10 µL of reaction containing 200 ng of PCR product, 20 U of DpnI (New England Biolabs) and Tango buffer (New England Biolabs). The digestion was carried out at 37ºC for 6 h. Afterwards, the DpnI was heat inactivated by incubating at 80ºC for 20 min. The DNA concentration were determined using a nanodropTM 2000c (Thermo scientific).The protocol to access the ligation of the *asp2ox* genes to the vector followed the recommendation of New England BioLabs for the NEBuilder HiFi DNA Assembly *i.e.* 60 ng of vector PCR product was incubated with 82 ng of *asp2ox* PCR product (ratio 1:3) in the presence of 10 µL of NEBuilder HiFi DNA Assembly Master Mix. The ligation was performed at 50ºC during 1 h. The final PCR ligated mixture (that will be mentioned as *asp2ox* gene library) was stored at -20ºC until use.

2.4.3 'Activity-on-plate' screening

Frozen electrocompetent KRX *E. coli* aliquots were transformed as described in section 2.1.3 but the volume of *asp2ox* gene library used was 2 µL *per* transformation instead of 1 µL described before for transformation with the plasmid. The transformed suspension was spread into LA petri dishes pre-supplemented with 100 µg/mL of ampicillin and 6 mM rhamnose. Dilutions were performed to ensure up to a maximum of 200 colonies *per* plate. The plates were incubated overnight (~17 h).
In the following day, all plates were numbered and the number of colonies in each plate counted. Colonies were replica-plated onto chromatography paper (Whatman) and the original culture-plate was re-incubated at 37ºC until colonies re-appeared (~ 6 h). For the first generation, the colonies on the filter papers were lysed by soaking the chromatography paper in a solution of 2 mg/ml of Lysozyme

(AppliChem) in 20 mM Tris-HCl, pH 7.6. The chromatographic papers were placed at 37ºC for 2 h in order to achieve the optimal temperature for the activity of lysozyme. For the second generation, instead of lysozyme, disruption was performed using the 40 % B-PER bacterial protein extraction reagent (Thermo-fisher) and the incubation was performed during 20 min at room temperature.
In both generations, after the incubation, the chromatographic papers were soaked in the reaction mixture containing 100 mM sodium phosphate buffer, pH 7.5, 1 mM AAP, 10 mM DCHBS, 8 U HRP and 0.5 M D-glucose. After this soaking, the development of the pink chromogen at room temperature indicates the presence of AsP2Ox activity.

2.4.4 Optimized 96-wells plates growth and screening

In the day after the 'activity-on-plate' screening, 96-deep-well plates were prepared by filling the edge wells, to prevent media evaporation, with 1 mL of bi-distillated H_2O and the remain 60 wells were filled with 400 µL of LB supplemented with 100 µg/mL of ampicillin. The wells B2 and C2 were the media contamination control and all other wells were inoculated by picking the positive AsP2Ox activity colonies from the re-grown plates of the 'activity-on-plate' (with sterile toothpicks). The pre-inocula was performed in 96-deep-wells plates covered with a sealing film and incubated at 37ºC, 750 rpm for 24 h. In the following day, new sterile 96-deep-well plates were prepared filling the edge with bi-distillated H_2O and the remaining 60 wells were filled with 900 µL of TB supplemented with 100 µg/mL of ampicillin. Next, 100 µL of pre-inocula was transferred from each well of the LB 96-deep-well cultures to the correspondent TB 96-deep-well plates. The plates were covered with a sealing film and cultures had grown for 3 h at 37ºC, 750 rpm at which time were induced with 12 mM rhamnose. Afterwards, the growths proceed overnight at room temperature. In the following day, the plates were centrifuged at 4ºC, 4000 rpm for 30 min on an Eppendorf 5810 R centrifuge. The supernatants were discarded and the plates with the cell pellets were stored at -80ºC until use. At the time the activity screening was performed, the plates containing the cell pellets were unfrozen and three cycles of N_2 freezing and 10 min thawing (at room temperature) were performed. After the last thaw, the cell pellet was resuspended with 200 µL of 20 mM Tris-HCl buffer at pH 7.6 supplemented with 2 mg/mL of lysozyme and the 96-deep-wells plates containing this resuspension were incubated during 20 min at room-temperature with 750 rpm. The plates containing the suspensions after the cell disruption were centrifuged on Eppendorf 5810 R centrifuge (4000 rpm, 30 min at 4ºC). The supernatants were collected (cell crude extracts) and used for enzymatic activity measurements. The enzymatic activity of each plate was tested by the HRP-AAP/DCHBS coupled assay by transferring 50 µL of cell crude extracts to a new 96-well microtiters containing 150 µL of reaction mixture: 0.1 mM of AAP, 1 mM of DCHBS, 8 U of HRP and D-glucose (0.5 M or 0.1 M for the first and second generation, respectively) in 100 mM phosphate buffer, pH 7.5. The progress of was followed by the increase of absorbance at 515 nm using a Synergy2 microplate reader (BioTek).

2.5 Directed evolution AsP2Ox hits characterization

2.5.1 pH profile and steady-state kinetics using HRP-AAP/DCHBS coupling assay

The procedure applied to determine the pH profile of the DE hit variants as well as the methodology applied to performed the steady-state kinetics to achieve the apparent steady-state parameters was similar than those described in sections 2.3.2 and 2.3.3.

2.5.2 Transient-state kinetics

The Transient-state kinetics was performed in a stopped-flow apparatus (TgK scientific) that was placed into an anaerobic chamber to work in anoxic conditions. All assays were performed at 25ºC. The routine detector used was a diode array (TgK scientific) that allows the acquisition of several spectra during time.
After the spectra acquisition, all traces of both oxidative and reductive half reactions were treated using Kinetic studio software (TgK scientific) and the data was adjusted to the monoexponential curve (Equation 1.1). Optimized adjustments were achieved using Solver Ad tool of Microsoft excel.

$$[P] = -A * exp^{-k_{obs} * t} + C$$

Equation 1.1 Formula of a monoexponencial function used for adjustment of traces obtained during stopped-flow experiments. where [P] is the FAD concentration, A is the amplitude of the exponential between time 0 min and infinite time, k_{obs} is the pseudo-first order constant, C the constant that expresses the absorbance at 460 nm when time goes to infinite and t is the time of reaction .

2.5.2.1 Reductive half-reaction

The buffer of the protein preparation was changed using a pre-calibrated 5 mL HiTrap desalting column (Sephadex G25 resin, GE healthcare Life sciences) inside of anaerobic glovebox. The loading volume of the protein preparation in the HiTrap column was 1.5 mL and the collection was performed with 2 mL deoxygenized 100 mM potassium phosphate buffer, pH 7.5 supplemented with 0.2 M of NaCl (for wild-type AsP2Ox) or 50 mM Tris-HCl buffer supplemented with 0.2 M of NaCl, pH 7.5 (for 1A1 AsP2Ox variant) or pH 8.5 (for 5D5 AsP2Ox variant). Dilutions were prepared to have protein preparations with $Abs_{460\ nm} \approx 0.08$ A.U. when fully oxidized.
The stopped-flow apparatus was pre-calibrated using the same deoxygenized buffer that was applied to prepare the protein preparation. D-glucose stock's solution (3 M) and dilutions were prepared inside of the anaerobic chamber with the same deoxygenized buffer that was applied to prepare the protein preparation.
The traces were obtained by loading the drive syringe with each D-glucose concentration and then shoot versus protein preparation that had been loaded in other drive syringe.

2.5.2.2 Oxidative half-reaction

Inside the anaerobic chamber, the protein preparation was reduced with approximately 33 µM of Glucose (color changed from yellow to colorless). Afterwards, protein preparations were transferred to a pre-calibrated 5 mL HiTrap desalting column (Sephadex G25 resin, GE healthcare Life sciences) in order to change the solution buffer of the protein. The loading volume of protein in HiTrap column was 1.5 mL and the collection was performed with 2 mL of deoxygenized 100 mM potassium phosphates buffer, pH 7.5 supplemented with 0.2 M of NaCl. Dilutions were prepared to have protein preparations with $Abs_{460nm} \approx 0.08$ A.U. when fully oxidized. In order to perform solutions with different concentrations of O_2 5-mL vials were pre-loaded with 3 mL of non-deoxygenized 100 mM potassium phosphates buffer, pH 7.5 supplemented with 0.2 M of NaCl. The different dilutions of O_2 were performed in a Hamilton syringe (gastight) by diluting the non-deoxygenized buffer with the deoxygenized buffer. As a preliminary approximation, it was assumed that the initial O_2 concentration in non-deoxygenized buffer was 250 µM. However, the real oxygen concentration in each dilution was

determined shooting the O_2 containing buffer dilutions versus 100 μM sodium dithionite solution (absorbance was followed at 315 nm and the acquisition was performed in a photomultiplier detector – TgK Scientific).
The spectra traces were obtained by shooting the reduced protein preparation pre-loaded onto the drive syringe versus each dilution of oxygenized buffer solution pre-loaded in the other drive syringe.

2.5.3 Steady-state kinetics following the O_2 consumption

In order to follow the AsP2Ox reaction by the O_2 consumption an Oxygraph apparatus was used. The 3 M stock solution of D-glucose was prepared in 100 mM potassium phosphates buffer, pH 7.5 (for the assays with wild-type and 1A1) or 50 mM Tris-HCl buffer pH 8.5 (for the assays with 5D5 AsP2Ox variant). Solution was deoxygenized by bubbling N_2. All enzymatic assays occurred in 1 mL containing 1 M D-glucose. The reaction mixture was shaken in a closed temperature-controlled chamber (37ºC). The oxygen concentration in the reaction chamber was different in each assay and it was pre-set by bubbling the 1 M D-glucose mixture with O_2 or N_2 gas. When the oxygen concentration stabilized in solution, the reaction was started by the addition of the AsP2Ox. The rate of O_2 consumption was obtained directly by the initial slope of reaction. Kinetic parameters were estimated (for wild-type and 1A1 AsP2Ox variant) by fitting the data directly in the Michaelis-Menten equation using OriginLab software. For 5D5 AsP2Ox variant, it was used the first-order approximation of the Michaelis-Menten equation ([S] « K_m) to calculate the catalytic efficiency.

2.6 Site-directed mutagenesis and characterization of variants

To construct AsP2Ox variants with single amino acids substitutions the site-directed mutagenesis (SDM) technique was used. Primers were constructed that completely pair with the template sequence except in one base that allowed the introduction of the desired mutation. The construction of the primers was performed with the help of SnapGene software. The plasmid pET-15b carrying the wild-type *asp2ox* gene was used as DNA template and the PCR carried out with the appropriated primers (Table 2.1). PCRs were performed in a thermal cycler in 50 μL reaction volumes containing 80 ng of DNA template, 1 μM of primers (forward and reverse for each mutation), 200 μM of dNTPs (NZYTech), NZYProof polymerase buffer, and 1.3 U of NZYProof polymerase (NZYTech). The conditions used for performing the PCR reactions were: 4 min initial denaturation at 95ºC, 20 cycles of 1 min at 95ºC, 1.5 min at 68ºC and 8 min at 72ºC. After that, the PCR had a final step of 10 min at 72 ºC. Five microliters of the amplified product was checked using agarose gel (1%) electrophoresis in a 40 min-run under an electrical field of 100 V (The presence of a strong band at around 7300 bp shows that the PCR was successful). The amplified product was digested with 10 U of DpnI (Thermo Scientific) at 37ºC for 5 h to eliminate the wild-type template. The digested PCR product was purified using Illustra GFX PCR DNA kit (GE Healthcare). The final elution during the purification was performed with 30 μL of milli-Q water. Five microliters of purified PCR product were used to transform electrocompetent *E. coli* KRX cells. The presence of the desired mutation(s) in the resulting plasmid and the absence of additional mutations in other regions of the insert was confirmed by DNA sequencing. To perform the double mutant Q295H/G366S the procedure was similar than those described before but instead of wild-type as DNA template, it was used the plasmid that carried the 1A1 variant, and the primers used were the ones that allow the introduction of the mutation Q295H.

The production and purification of each mutant was performed as described before (section 2.2.2), and pH profile analysis and the steady-state kinetics for each variant was performed similarly to the previously mentioned for other AsP2Ox variants (described in section 2.3.2 and 2.3.3).

Table 2.1 - Primers used in the site-directed mutagenesis for the construction of different mutants. Fwd- primer forward; Rev- primer reverse. The nucleotides in bold and underlined correspond to the base substitutions that allow the desire mutations.

Mutation		Primer
A75T	Fwd	5'-GGGTCCCGGT**A**CCGGTGCTGCAACAGTG-3'
	Rev	5'-CACTGTTGCAGCACCGG**T**ACCGGGACCC-3'
A206T	Fwd	5'-GCAGGATGGC**A**CCCTCGTATGGTCCGGCTC-3'
	Rev	5'-GAGGCCGGACCATACGAGGG**T**GCCATCCTGC-3'
Q295H	Fwd	5'-CTGAACGACCA**T**GCGCAGGTGGTGTTCGCG-3'
	Rev	5'-CGCGAACACCACCTGCGC**A**TGGTCGTTCAG-3'

3. Results and Discussion

3.1 Development of useful tools

The first part of results in this thesis are a set of different non-related experiments which were performed to test and optimize routine conditions and methods that are relevant for the success of the DE procedures.

3.1.1 Selection of *E. coli* strain for large-scale production

Optimal large-scale growth of recombinant *E. coli* strains is important to allow production of large quantities of cells overproducing the protein of interest for further purification, kinetic and biochemical characterization.

The routine protocol used in the laboratory for large-scale production of AsP2Ox variants was based on cell growth in 5 L-Erlenmeyers containing 1 L of LB medium and the *E. coli* expression strain that had been used was BL21 star due the high production yields previously obtained.

However, some reports of the student that worked previously with AsP2Ox and also my results **(**Figure S6.1**)** showed that this protocol did not provide reproducible growth.

In all growths **(**Figure S6.1**)**, the culture starts to grow and concomitantly increase of the $OD_{600\ nm}$ but *E. coli* cells died at an early stage of growth (the observation of culture media suggest the existence of aggregates that represent lysed cells). Since we previously know that the expression of *asp2ox* gene was leaky, due protein of interest was produced in non-induced cells, we had hypothesized that the non-regulation of gene expression, at an early stage of growth, could lead to AsP2Ox production. This can oxidize sugars in the cytoplasm of cells, releasing the H_2O_2 product or other toxic species that kill *E. coli* cells.

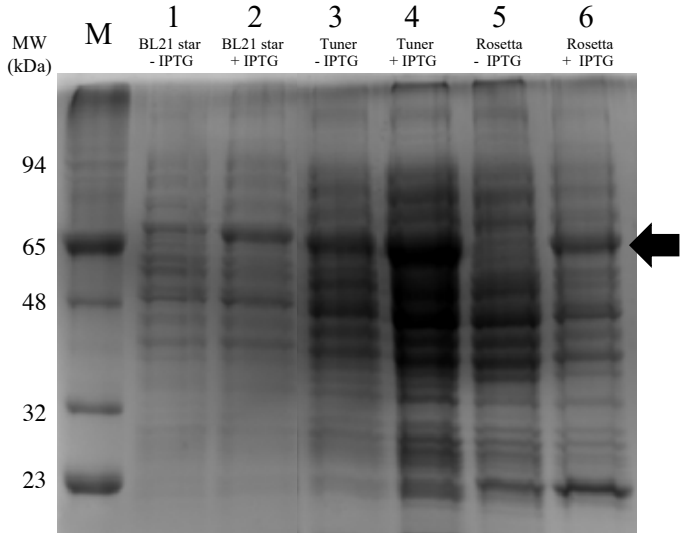

Figure 3.1 SDS-PAGE of cell crude extracts of different *E. coli* strains after growing at small-scale (50 mL). M is the molecular mass marker. Crude extracts of *E. coli* BL21 star strain without induction (lane 1) and induced with IPTG (lane 2); Crude extracts of *E. coli* Tuner strain without induction (lane 3) and induced with IPTG (lane 4); Crude extracts of *E. coli* Rosetta strain without induction (lane 5) and induced with IPTG (lane 6). The protein concentration was determined by the Bradford method and the volume loaded in each well was calculated to correspond ~ 20 μg of protein. The black arrow indicates the AsP2Ox protein band (~64 kDa).

To test this hypothesis, we had tested several *E. coli* host strains (BL21 star strain as control, Tuner and Rosetta strains) by growing them in small-scale (in 50 mL of media) in the presence and absence of

IPTG. The BL21 star strain has an increment in mRNA stability which can result in higher levels of basal expression and thus it is not in general, suitable to express toxic genes, the Tuner strain is indicated for cases when it is desirable a homogeneous expression level that can be adjusted by the IPTG concentration, and the Rosetta *E. coli* strain is a strain containing an extra plasmid that supplies tRNAs that are less abundant in *E. coli*.

E. coli strains were grown in two independent 50- mL cultures, one induced with IPTG and the other non-induced (Figure 3.1). The cell growth was monitored following the optic density at 600 nm (Figure S6.2).

The analysis of the SDS gel (Figure 3.1) revealed that the BL21 star has the band corresponding to AsP2Ox at ~64 kDa in cell extracts of induced as well of non-induced cells which suggest leaky expression of AsP2Ox, although the concentration in non-induced is slightly lower when compared with induced growth. Similar results were obtained when AsP2Ox is produced in the Tuner strain, even though the protein production yields are higher than in BL21 star which can represent an advantage in certain conditions. Importantly, in the Rosetta strain, the ~64 kDa is not present in crude extracts of non-induced cells while in induced cells a band at that the AsP2Ox molecular weight can be observed, with approximately the same thickness than the one obtained for (induced) BL21 star strain indicating that the protein was expressed approximately at the same yields. Overall our results indicate that the expression of the *asp2ox* gene, in the Rosetta strain, is fine regulated and just starts after the addition of IPTG to the cultivation media suggesting that this strain could be a good candidate for large-scale production.

Next, we have tested the production of AsP2Ox in both the Tuner (that could represent a plus in protein production yields) and Rosetta (that showed to be a well-regulated strain for the production of the interest protein) strains at large-scale.

Because the large-scale production aims to get the maximum of cells possible, instead of the typical 1 L of growth performed before, new cultivation flasks (Corning® 5L Baffled PETG) were tested that allow cell growth in 2.5 L of LB media (Figure 3.2).

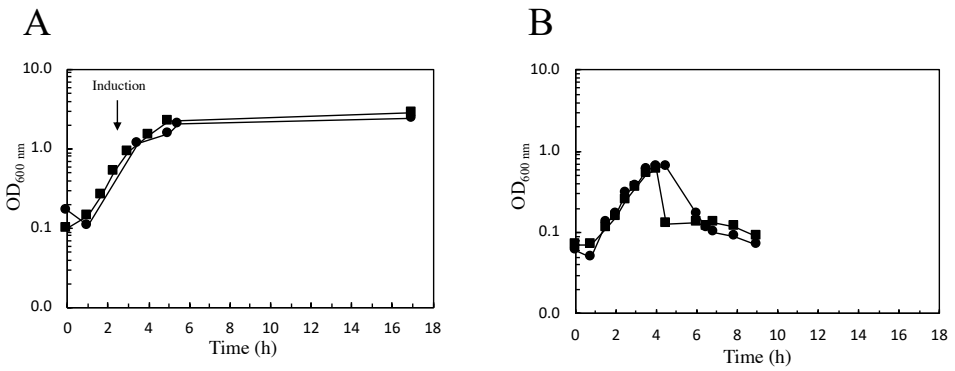

Figure 3.2 Growth curves of two distinct *E. coli* strains carrying the wild-type gene of AsP2Ox in 2.5 L-scale. In (A) the *E. coli* Rosetta strain was used and the induction of plasmid expression containing the *asp2ox* gene with 100 μM of IPTG ($OD_{600\ nm} \simeq 0.8$ A.U.) are marked with a black arrow. In (B) Tuner *E. coli* strain was used and the induction was not performed because the cells died before reaching $OD_{600\ nm}$ of ~0.8 A.U.. All cultures started with an initial $OD_{600\ nm}$ of 0.1 A.U.. The black symbols represent the data obtained by monitoring the optical density at 600 nm. After induction growing temperature was changed from 37ºC to 25ºC.

As can be seen, both growths that used *E. coli* Rosetta as expression host grew quite well, were induced with IPTG at $OD_{600\ nm} \simeq 0.8$, and after 17 h of cultivation, the presence of the AsP2Ox was tested by SDS analysis and also activity assays in crude extracts (data not shown). In contrast, the two cultures performed using *E. coli* Tuner died before induction which means that Tuner is not a suitable expression strain for large-scale production.

These results support the hypothesis that the leaky expression in the early stage of growth (in strains that do not regulate well the plasmid expression) could culminate in cell death. However, it is not well understood, with this simple approach, why Rosetta strain allows for a tighter regulation of heterologous gene expression as compared with Tuner and BL21 star strains and the reason why all strains grew well and produce the protein of interest at a small-scale but BL21 star and Tuner died when the growth is scaled-up.

3.1.2 Optimization of the detection method of AsP2Ox enzymatic activity

As mentioned in the Introduction, the AsP2Ox catalyzes the regioselective C2 oxidation of several sugars releasing the correspondent keto-sugars. During this process, the FAD cofactor of the enzyme becomes reduced and the electron transfer process ends when the enzyme finds a molecule that can act as an electron acceptor. Because this work aims to improve this bacterial P2Ox to D-glucose and dioxygen, the O_2 will be the desired electron acceptor that provides H_2O_2 when is reduced by enzyme activity (Figure 3.3A).

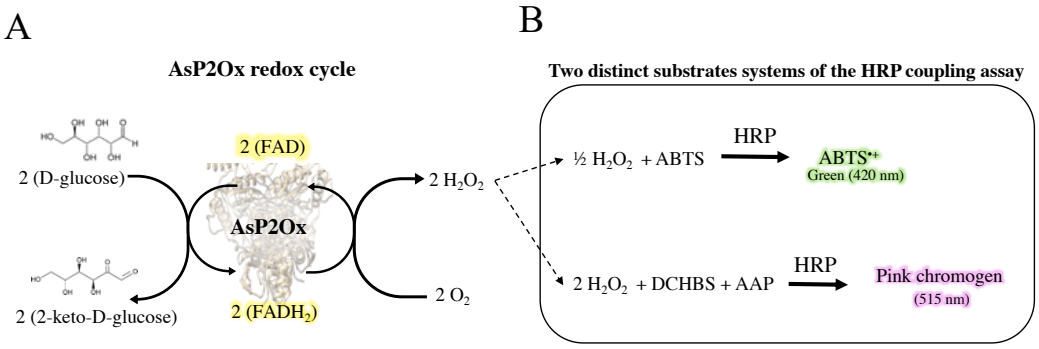

Figure 3.3 Overall scheme of the catalytic cycle of AsP2Ox and of coupled reaction assay to measure (indirectly) its activity. (A) Scheme of the catalytic redox cycle of AsP2Ox using D-glucose as electron donor and O_2 as electron acceptor. (B) routine HRP coupled assay to measure (indirectly) the activity of AsP2Ox using two distinct HRP substrate systems: on top ABTS is used being oxidized to $ABTS^{\bullet+}$ in the presence of H_2O_2 generated by AsP2Ox activity (the green characteristic colour of $ABTS^{\bullet+}$ can be followed spectrophotometrically at 420 nm). On the bottom, AAP and DCHBS substrates are used by HRP, in the presence of H_2O_2, to generate N-(4-antipyryl)-3-chloro-5-sulfonate-p-benzoquinone-monoimine (that will be referred as pink chromogen) and can be followed spectrophotometrically at 515 nm.

The routine method to determine the activity of P2Ox using O_2 as electron acceptor is based in a reaction coupled assay with HRP and ABTS. In this coupled assay, HRP uses its substrate (ABTS) and the hydrogen peroxide (released by the P2Ox activity) to generate a dark green compound ($ABTS^{\bullet+}$) that can easily be followed spectrophotometrically at 420 nm (Figure 3.3B)

One of the drawbacks in using coupled assays relates to the higher complexity of the reaction mixtures and lower control of reaction conditions. Additionally, some references suggest that $ABTS^{\bullet+}$ could be an electron acceptor of the P2Ox catalytic cycle competing with O_2. Consequently, the P2Ox activity measured for the O_2 using the HRP-ABTS system could be higher than the measured because $ABTS^{\bullet+}$ will compete with O_2, the chromogenic green compound ($ABTS^{\bullet+}$) can be bleached to the colorless form (ABTS) during the catalytic cycle leading in non-reliable results (Figure 3.4A – top scheme)**.**

To test the capability of AsP2Ox to use the $ABTS^{\bullet+}$ as electron acceptor a spectrophotometric assay was performed using 1 M D-glucose and $ABTS^{\bullet+}$ (the utilization of this compound as electron acceptor by AsP2Ox should turn $ABTS^{\bullet+}$ to ABTS which is colorless resulting in a decrease of absorbance at 420 nm). This experiment was performed in anaerobioses (where the $ABTS^{\bullet+}$ is the only possible electron acceptor) and in aerobioses (where a competition between $ABTS^{\bullet+}$ and O_2 can occur) **(**Figure 3.4A).

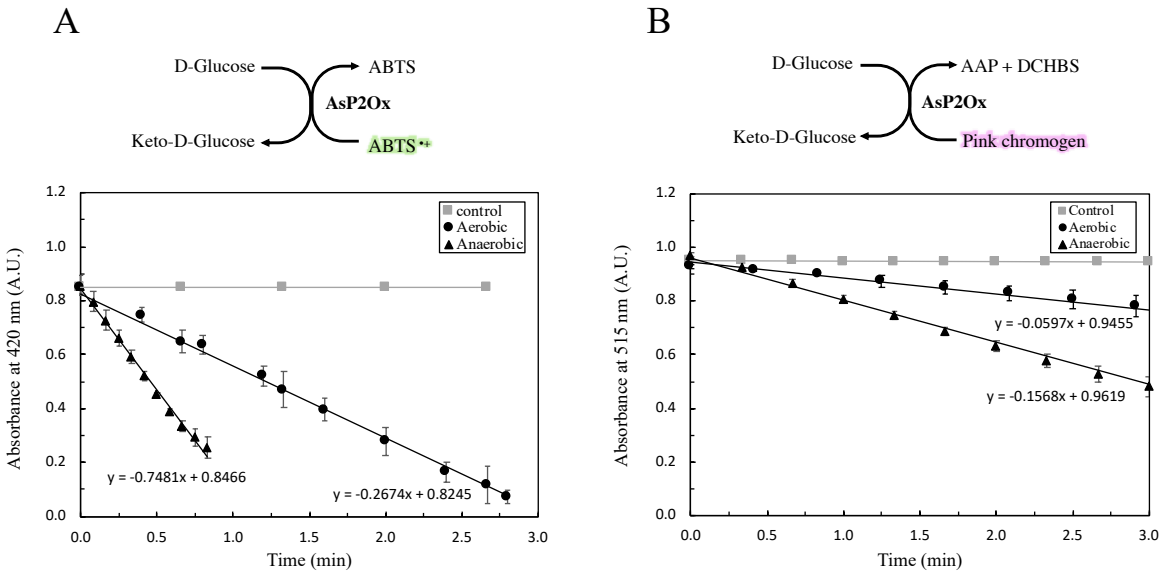

Figure 3.4 Preliminary spectrophotometric assay to test the bleaching of oxidized chromogens formed during wild-type AsP2Ox reaction using D-glucose as electron donor. (A) AsP2Ox reaction using the $ABTS^{\bullet+}$ as electron acceptor in the presence of oxygen (black circles) and in absence of oxygen (black triangles). (B) AsP2Ox reaction using the pink chromogen as electron acceptor in the presence of oxygen (black circles) and in the absence of oxygen (black triangles). In both graphics, the grey squares represent a control experiment without the addition of protein (similar data was obtained for the control without the addition of D-glucose – not shown). The equation below each data set represent the linear regression of the raw data (solid lines) and the schemes on top of each graphic represents the chromogen bleaching hypothesis to be tested. All reactions were performed in 100 mM sodium phosphates buffer pH 7.5 in the presence of 1 M of D-glucose and at 37ºC.

The results obtained in the absence of oxygen revealed that $ABTS^{\bullet+}$ is bleached to ABTS (decrease of absorbance at 420 nm) which means that $ABTS^{\bullet+}$ is an electron acceptor of AsP2Ox. In the presence of oxygen, the rate of bleaching is almost 3-fold lower because there is another electron acceptor (O_2), however, the bleaching rate is still high which indicates that the HRP-ABTS method is not suitable to measure the AsP2Ox activity.

Consequently, a new substrate system was tested for HRP using AAP and DCHBS substrates to replace ABTS. These two compounds in the presence of H_2O_2 released by the AsP2Ox activity and by the action of HRP are converted into N-(4-antipyryl)-3-chloro-5-sulfonate-p-benzoquinone-monoimine that shows a pink color (the reason why this compound is called during this thesis as pink chromogen) that can be followed at 515 nm in a spectrophotometer (Figure 3.3B).

In the literature, there are not references that the pink chromogen can be used as electron acceptor by P2Oxs. However to be confident that this system can be used to measure accurately the AsP2Ox activity without the interference observed in the HRP-ABTS system, a spectrophotometrical assay was performed similarly to the one described above where the pink chromogen bleaching was followed during the AsP2Ox assay in the presence and absence of O_2 (Figure 3.4B).

The results show both in the presence or absence of dioxygen, the pink chromogen can indeed act as an electron acceptor of the AsP2Ox, but the bleaching rate is, in both situations, ~5-fold lower than those obtained for $ABTS^{\bullet+}$.

Overall, the results obtained show that the affinity of AsP2Ox for the pink chromogen is lower than for $ABTS^{\bullet+}$ which means that HRP-AAP/DCHBS is a more suitable method to measure the AsP2Ox activity using the HRP coupling assay, even if a small chromogen bleaching is observed by the action of AsP2Ox, that could result in activities slight underestimated activity measurements. To counteract this issue, the activity measurements during this thesis were obtained from the initial reaction rates *i.e* when the concentration of pink chromogen is low.

3.1.3 Re-characterization of wild-type AsP2Ox using the HRP-AAP/DCHBS method

The steady-state kinetics of AsP2Ox for D-glucose and O_2 described in [24] had been performed using HRP-ABTS method, however as it was proved in the section before the HRP-ABTS is not a suitable enzymatic assay method, the reason why the pH profile as well as the steady-state characterization of wild-type AsP2Ox was re-analyzed using the HRP-AAP/DCHBS method.
By the analysis of Figure 3.5 it can be seen that the optimum pH for AsP2Ox activity is between 7 and 7.5, however for all kinetic characterization performed a buffer at pH 7.5 was used because D-glucose tends to slightly decrease the pH of the reaction mixture.

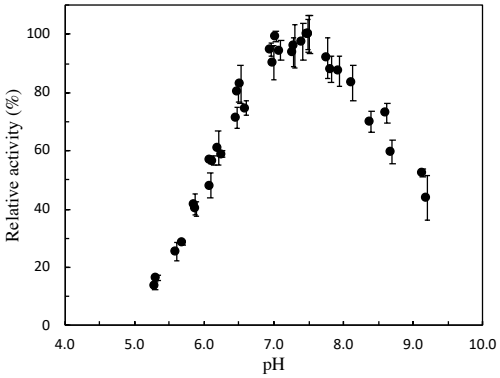

Figure 3.5 pH profile of wild-type AsP2Ox. The activity method used was HRP-AAP/DCHBS coupled assay. The data suggest that the optimal pH range is between 7.0 and 7.5. The assays were performed in presence of 0.3 M of D-glucose at 37ºC and the buffer used was Briton and Robinson (pH range 5 to 9). The pH of the reaction mixture was verified using a pH electrode. The relative activity was calculated considering the maximum of activity (optimal pH) as 100 %.

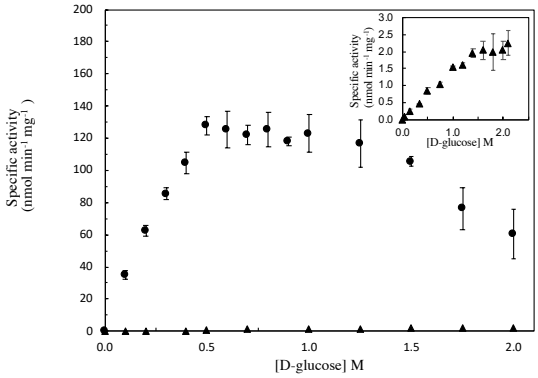

Figure 3.6 Comparison of steady-state kinetics obtained using the two substrate systems of HRP. The black circles represent the data obtained using HRP-AAP/DCHBS coupled assay (at pH 7.5) and the black triangles are the data obtained using HRP-ABTS coupled assay (at pH 6.5). The data from HRP-ABTS coupled assay was collect by the previous student of the Lab. Both assays were performed at 37ºC in oxygenized 100 mM of sodium phosphates buffer.

In Figure 3.6 steady-state curves are displayed comparing the results using the HRP-ABTS and the HRP-AAP/DCHBS coupled assays. It is possible to observe a change in the curves shape from a linear to a Michaelis-Menten curve and the values of the activities increased 1-2 orders of magnitude which suggest that the previous results obtained with HRP-ABTS were strongly underestimated.
Using the HRP-AAP/DCHBS coupled reaction it was also performed the steady-state kinetics for other sugars (D-xylose, D-ribose, L-arabinose and D-galactose) using the O_2 as electron acceptor (Table 3.1**).**

The data suggest, between the tested sugars, the D-glucose is the preferred substrate with a catalytic efficiency of 0.51 ± 0.10 M^{-1} s^{-1}.

Table 3.1 Apparent steady-state kinetic parameters of wild-type AsP2Ox for different sugar substrates (D-glucose, D-xylose, D-ribose, L-arabinose and D-galactose), using O_2 as electron acceptor. The data was obtained with HRP-AAP/DCHBS coupled assay at 37ºC in 100 mM sodium phosphate buffer at pH 7.5 and the routine reaction mixture contained 0.1 mM of AAP, 1 mM of DCHBS and 8 U of HRP. The kinetic parameters were determined by OriginLab by fitting the data directly on the Michaelis-Menten equation.

Substrate	K_m (M)	k_{cat} (s^{-1})	k_{cat}/K_m (M^{-1} s^{-1})
D-glucose	0.37 ± 0.13	0.18 ± 0.01	0.51 ± 0.10
D-xylose	0.72 ± 0.30	0.12 ± 0.02	0.19 ± 0.08
D-ribose	0.20 ± 0.09	0.01 ± 0.00	0.07 ± 0.04
L-arabinose	0.42 ± 0.14	0.02 ± 0.00	0.05 ± 0.03
D-galactose	0.51 ± 0.26	0.02 ± 0.00	0.04 ± 0.03

3.1.4 Characterization of AsP2Ox variants obtained previously in the course of DE

As it was mentioned before the evolution of AsP2Ox in MET Lab already started by a student that found a variant (named CM3) that had 10-folds higher catalytic efficiency using D-glucose as the electron donor. The screenings performed by that student, for AsP2Ox activity was based in spectrophotometrically assays in crude extracts using the HRP-ABTS method in 96-wells plates. Due the fact of the HRP-ABTS had been used as activity detection method, some doubts arise on the reliability of the evolution that had been performed.

To start a new directed evolution cycle, one must be confident about the variant that should be used as a parent, therefore steady-state kinetics of 2C9* (intermediate variant) and CM3 (hit variant) was performed using the HRP-AAP/DCHBS method (Table 3.2).

Table 3.2 Apparent steady-state kinetic parameters of wild-type, 2C9* and CM3 AsP2Ox variants using D-glucose as electron donor and O_2 as electron acceptor. The data was obtained with HRP-AAP/DCHBS coupled assay at 37ºC in 100 mM sodium phosphate buffer at pH 7.5 and the routine reaction mixture contained 0.1 mM of AAP, 1 mM of DCHBS and 8 U of HRP. The kinetic parameters were determined by OriginLab by fitting the data directly on the Michaelis-Menten equation. ND means not determined.

Variant	K_m (M)	k_{cat} (s^{-1})	k_{cat}/K_m (M^{-1} s^{-1})
Wild-type	0.37 ± 0.13	0.18 ± 0.01	0.51 ± 0.10
2C9*	0.52 ± ND	0.04 ± ND	0.08 ± ND
CM3	0.35 ± ND	0.03 ± ND	0.09 ± ND

The analysis of the apparent steady-state parameters shows that the turnover number, k_{cat} (which is a measure of the rate of product formation) of both variants is ~5/6-fold lower than the wild-type which results in catalytic efficiencies, k_{cat}/K_m, 5/6-folds lower. These results suggest that during the evolution procedure performed by the previous student the enzyme did not evolve as desired (Figure 3.7).

Considering these results, we concluded that the best option was to disregard the variants obtained before and start fresh using wild-type AsP2Ox as parent of a new generation of directed evolution.

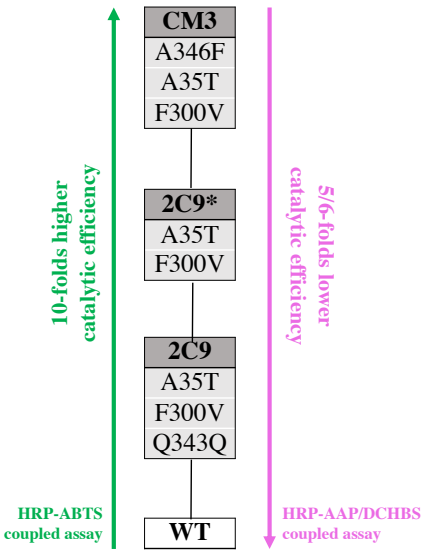

Figure 3.7 Evolution tree of AsP2Ox with variants that were performed previously on the MET Lab. In green is represented the overall comparison between wild-type (WT) and the last hit variant (CM3) obtained using the HRP-ABTS coupled assay and in pink is the overall comparison between the same variants using the HRP-AAP/DCHBS coupled assay.

3.2 Directed evolution of AsP2Ox

The most challenging steps in directed evolution technique is the achievement of good screening (and/or selection) methods. The screening should be fast, sensitive enough and preferable high throughput allowing the analysis of a large number of variants in low time frames. For the DE evolution of AsP2Ox, two different approaches were used in the screening: 'Activity-on-plate' and 96-wells plate liquid screenings.

3.2.1 Screenings optimization

3.2.1.1 'Activity-on-plate' screening

The 'Activity-on-plate' screening, which main steps are described in Figure 3.8, is a method that was developed in MET Lab and uses the spatially separated variants principle. In this screening, the library of *asp2ox* gene variants is used to transform *E. coli* cells that are plated on LA plates (pre-supplemented with the appropriate antibiotics and with the inducer which allows *in situ* protein production during the colonies growth). In the day after, the colonies are transferred to a chromatographic paper by replica plating and the initial solid media plates are incubated to allow re-growing the colonies. The chromatographic paper is soaked in a lysis buffer (that contains a lysis detergent for protein extraction or lysozyme) to disrupt the bacterial cell wall, and after, they are soaked in reaction mixture that contain all necessary components for the development of color. During the AsP2Ox evolution the reaction mixture contained D-glucose, HRP, AAP and DCHBS, and the development of a pink color on the lysed colonies, in the chromatographic papers, indicates enzyme activity. The intensity of color and the rate of color development is intrinsically related to the enzyme variant which means that an intense color suggests an improved variant for activity. The selected positive variants identified in LA plates are further screened after growth in liquid media.
The 'Activity-on-plate' represents an excellent methodology to screen a high number of variants providing a qualitative analysis which is a plus to decrease the number of variants to be screened in

liquid 96-wells plates, although this method is just applicable when the enzymatic assay used develops color.

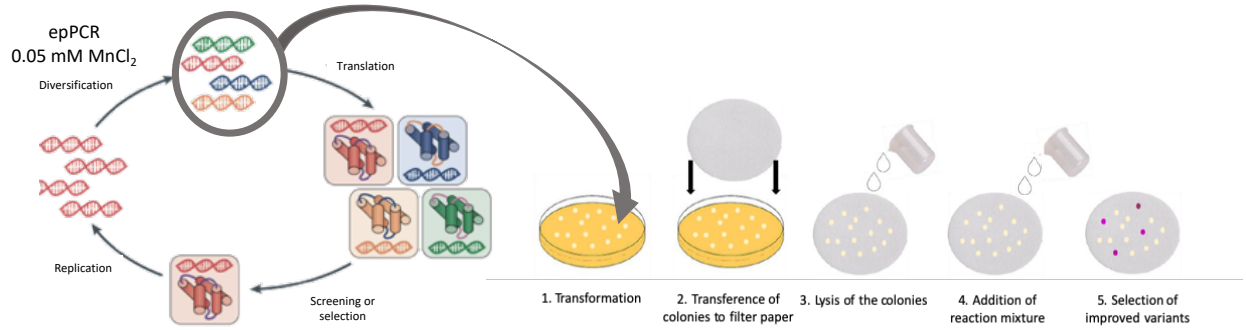

Figure 3.8 Directed evolution main steps and high throughput 'Activity-on-plate' screening procedure. The general scheme of a directed evolution protocol which includes the diversification of the parent gene using epPCR (with [$MnCl_2$]= 0.05 mM), translation of each variants and screening of all of them (on left - Adapted [60]), and overview of 'Activity-on-plate' screening used during AsP2Ox evolution (on right). For 'Activity-on-plate' screening, the variant genes from the epPCR are used to transform *E. coli* cells and the gene expression coding for the desired protein will occur simultaneously with the growth of colonies. In the day after, the colonies are transferred to chromatographic paper and these are soaked in a lysis buffer to disrupt the cells and the enzyme activity, when filters are soaked in the reaction mixture is observed after development of color indicative of enzymatic reaction. The improved variants show more intense color.

In other cases, this approach, due to high variance of the screening, favored for example by insufficient disruption of the bacteria cells, does not allow to select the presumably improved variants but only the colonies that contain the protein of interest which is still advantageous due the fact that during the library construction some vector self-assemble without the *asp2ox* gene.
The validation of this screening is qualitative and needs to be performed before each round of evolution by transforming *E. coli* with the plasmid containing the gene of the enzyme variant that will be the parent of the following generation. All procedures are the same as described before and the process is validated when all lysed colonies on the chromatographic paper shows a low and similar intensity of color).

3.2.1.2 96-wells plates liquid screening

The liquid media screening is a quantitative approach and needs validation to reach the conditions that can easily allow the distinction between an improved variant and its parent, minimizing the selection of false positives. During the optimization of this screening, one of the objectives is to reduce the coefficient of variance (CV) of the system; the CV is an indicator of dispersion or cohesion of the system and reflects the reproducibility of the assay.
To develop, validate and implement this methodology, several experiments need to be performed at the level of cell growth, protein production, cell lysis, and activity screening assays in 96-wells plates. Usually, the optimization and validation are performed using microtiters plates whereas *E. coli* carrying the gene of the parent variant of the following generation is grown. In this thesis, the variant used for optimization was CM3 instead of wild-type, however when the best combination of conditions was found additional plates inoculated with wild-type were performed to check if the CV for total activity is kept low.
In this optimization, two variables were tested, namely the cell disruption method and the *E. coli* host strains in typical 96-wells microtiters and 96-deep-wells plates.

The main difference between the typical microtiters and the deep-wells plates are the higher oxygen concentration of the cultivation media in 96-deep-wells which supports higher cell yields and protein production levels. Additionally, due to the fact of the 96-deep-wells have higher volume of cultivation media, the number of cells obtained is higher than using the conventional microtiters which can be a plus for detecting enzymes showing low activity.

The first optimization process performed was the disruption method. For that, *E. coli* BL21 star was grown harboring the plasmid carrying the gene coding for the CM3 variant in microtiters or the deep-wells plates and after growth, the recovered cell pellets were disrupted using four different methods (Table 3.3)**.**

Table 3.3 Optimization of the method of cell disruption using liquid screening in 96-wells plates. Two different systems of cell cultivation were performed (growth in 200 μL and in 1 mL media). The optical density at 600 nm for pre-inocula and for the final culture was measured to check the variance of the systems in terms of cell cultivation. The total activity was performed using the HRP-AAP/DCHBS detection method with crude cell extracts after the disruption using 40 % B-PER detergent, 2 mg/mL of lysozyme, freeze in liquid nitrogen/thaw at room temperature or freeze at -80ºC/thaw at 37ºC. The *E. coli* strain used was, in all cases, the *E. coli* BL21 star expressing the gene coding for the CM3 variant. The reaction mixture to test the enzymatic activity contained 1 M of D-glucose 1 mM of AAP, 10 mM of DCHBS, 8 U of HRP and the assays were performed at 25ºC and monitored at 515 nm. For all the conditions tested only one plate was tested and the coefficient of variance (CV) corresponds to the variation within the plate tested. ND represent not detect activity.

		Growth in 200 μL (96-wells microtiters)						**Growth in 1 mL (96-wells Deep wells plate)**					
		OD_{600nm} Pre-inocula	CV (%)	OD_{600nm}	CV (%)	Total Activity (nmol min^{-1})	CV (%)	OD_{600nm} Pre-inocula	CV (%)	OD_{600nm}	CV (%)	Total Activity (nmol min^{-1})	CV (%)
Method of disruption	B-PER	0.6 ± 0.04	6	0.8 ± 0.1	8	1.2 ± 0.5	42	1.1 ± 0.1	5	1.6 ± 0.3	18	1.8 ± 0.6	30
	Lysozyme 2 mg/mL	0.6 ± 0.04	6	0.8 ± 0.1	11	ND	-	1.1 ± 0.1	5	1.5 ± 0.2	10	0.4 ± 0.2	40
	Freeze/Thaw (LN_2)	0.6 ± 0.04	6	0.8 ± 0.1	10	ND	-	1.1 ± 0.1	5	1.3 ± 0.2	14	ND	-
	Freeze/Thaw (-80°C)	0.6 ± 0.04	6	0.8 ± 0.1	12	ND	-	1.1 ± 0.1	5	1.2 ± 0.2	15	ND	-

The first method was a chemical disruption using the commercial B-PER® solution for protein extraction. The second method tested was an enzymatic one that uses lysozyme, an enzyme that catalyzes the hydrolysis of β (1→4) linkages between the N-acetylmuraminic acid and the N-acetyl-D-glucosamine residues of peptidoglycan present in bacterial cell walls. In *E. coli,* lysozyme weakens the cell wall and an osmotic effect can lead to cell disruption with the consequent cross of proteins to outside of cells [75]. The low-temperature physical methods putatively weaken the bacterial membrane/wall and open small pores that allow soluble overproduced proteins to be released without destroying the cells [76]. Within the low-temperature physical methods two were tested, in the first, the cells were submitted to three cycles of freezing with liquid nitrogen following by thawing at room temperature and, in the second method tested, cells were subjected to three cycles of freezing at – 80ºC for 15 min and then thawing at 37ºC for 5 min.

The results show that the variance within the pre-inoculum and cell growth is low (between 5-6 % for the pre-inocula and 8-18 % to growth) which means that all wells of one plate have almost the same number of cells (Table 3.3). B-PER was the only method that allows the AsP2Ox activity measurement in both microtiters and the deep-wells systems. Additionally, it was the method that provided the lower CV when 96-deep-wells plates were used.

Therefore, it was concluded that cell production in deep-wells and cell disruption with B-PER constitute a good combination of conditions to use in DE liquid screenings.

Next, we have tested two different *E. coli* host strains (BL21 star and KRX) **(**Table 3.4**).**

Table 3.4 Optimization of *E. coli* expression strain for directed evolution liquid screening in 96-wells plate. Two different systems of cell cultivation were performed (growth in 200 μL and in 1 mL). The optical density at 600 nm for pre-inocula and for the final culture was measured to check the variance of the systems in terms of the number of cells. The *E. coli* strains tested were BL21 star and KRX carrying the CM3 variant of AsP2Ox. The total activity was performed using the HRP-AAP/DCHBS detection method with crudes cell extracts after the disruption with 40 % B-PER detergent. The reaction mixture to test the activity contained 1 M of D-glucose 1 mM of AAP, 10 mM of DCHBS, 8 U of HRP and the assays were followed at 515 nm at 25 ºC. For all conditions tested only one plate was used per condition and the coefficient of variance (CV) corresponds to the variation within the plate tested.

		Growth in 200 μL (96-wells microtiters)						**Growth in 1 mL (96-wells Deep wells plate)**					
		OD_{600nm} Pre-inocula	CV (%)	OD_{600nm}	CV (%)	Total Activity (nmol min^{-1})	CV (%)	OD_{600nm} Pre-inocula	CV (%)	OD_{600nm}	CV (%)	Total Activity (nmol min^{-1})	CV (%)
***E. coli* expression strain**	BL21 star	0.6 ± 0.04	6	0.8 ± 0.1	8	1.2 ± 0.5	42	1.1 ± 0.1	5	1.6 ± 0.3	18	1.8 ± 0.6	30
	KRX	0.6 ± 0.2	26	0.8 ± 0.2	28	0.5 ± 0.6	121	1.0 ± 0.1	13	1.4 ± 0.2	12	4.7 ± 0.7	15

The results show that the final $OD_{600\ nm}$ in the microtiters plate that contain the KRX as expression strain is very variable (CV of 26 % in pre-inoculum and 28 % in the culture) and as consequence the total activity measured had a too high CV. The utilization of KRX as host strain growing in 96-deep-wells plate results in the lowest CV. The KRX strain represents an additional advantage comparing with BL21 star because it can be directly used for plasmid extraction without the need to transform in other strain as it happens with BL21 star.

Overall the results show that the most suitable process involves growing of KRX recombinant cells grown in a deep-wells plate followed by cell disruption with B-PER. However, since B-PER is an expensive commercial detergent with unknown composition an additional assay was performed to test the interference of this detergent on the catalytic cycle of AsP2Ox (Figure S6.3). The results revealed that some components in B-PER solution can act as electron donors of AsP2Ox invalidating the utilization of this detergent. Results in Table 3.3 show that the use of lysozyme can somehow replace B-PER as disrupting agent.

Table 3.5 Final validation of optimized directed evolution procedure for liquid media screenings in 96-wells plates. Three plates were performed in the same conditions using *E. coli* KRX as host strain (carrying the wild-type gene of AsP2Ox). The total activity was performed using the HRP-AAP/DCHBS coupled assay with crude cell extracts after the disruption with three cycles of freeze in liquid nitrogen/thaw at room temperature followed by lysis with 2 mg/mL of lysozyme. The reaction mixture to test the activity contained 1 M of D-glucose 1 mM of AAP, 10 mM of DCHBS, 8 U of HRP and the assays were followed at 515 nm at 25 ºC. The coefficient of variance (CV) corresponds to the variation within the plate tested.

	OD_{600nm}	CV (%)	Total Activity (nmol min^{-1})	CV (%)
Plate 1	0.9 ± 0.1	10	0.51 ± 0.05	10
Plate 2	1.0 ± 0.1	13	0.66 ± 0.12	18
Plate 3	1.0 ± 0.1	10	0.59 ± 0.12	23

To re-validate the screening methods KRX recombinant cells producing wild-type AsP2O were grown in 96-deep-wells plates and the collected pellets were disrupted using the conjunction of two methods: three cycles of freeze in liquid nitrogen / thaw at room temperature followed by enzymatic disruption with lysozyme **(**Table 3.5**)**.

The results in Table 3.5 show that the CV obtained for the total activity in the three plates varies between 10 % and 23 % which is lower enough to be used in DE libraries screenings.

3.2.2 First generation of directed evolution

When the screening methods were optimized the directed evolution of wild-type AsP2Ox started. A library of variants was constructed by epPCR using 0.05 mM of $MnCl_2$ and after ligation of gene variants to the vector a transformation of the library in KRX *E. coli* cells was performed.
Using the 'Activity-on-plate' high-throughput assay a mutant library of ~7,300 AsP2Ox variants was screened (an example of 'Activity-on-plate' screening is showed in Figure 3.9).

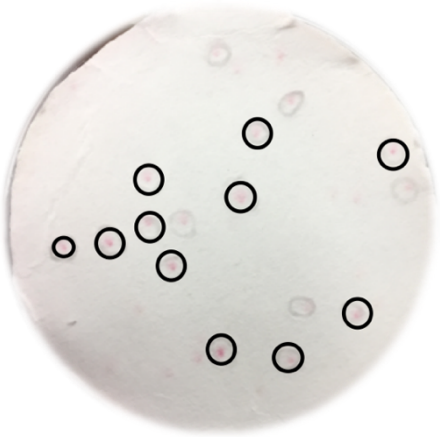

Figure 3.9 Example of an 'Activity-on-plate' screening performed during the evolution of AsP2Ox. The variants selected for 96-wells plate liquid screening are marked with a black circle

From the 7,300 tested, 95 colonies showed higher activity than the parent and were transferred to 96-deep well plates.
The 96-wells plate quantitative analysis of the 95 variants was performed by the HRP-AAP/DCHBS coupling assay using crude extracts obtained after cell disruption with 3 cycles of N_2/thaw followed by lysozyme and the activity of each variant was compared with the activity of the parent (wild-type AsP2Ox) allowing to calculate the relative activity Figure 3.10**.**

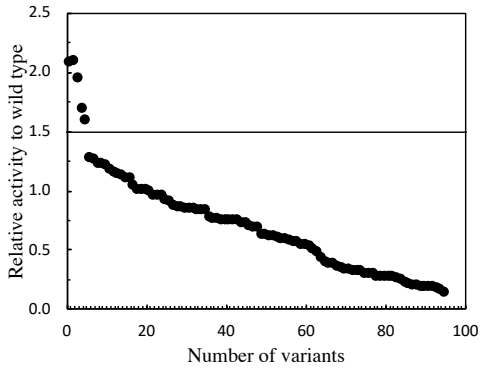

Figure 3.10 Activity of 95 variants from the first generation relative to wild-type after the first 96-wells plate liquid screening. The horizontal line at relative activity 1.5 represents the threshold used to select the variants for new rescreening in liquid medium. The relative activity of the variants is plotted in descending order.

From this screening, 6 variants showed relative activity higher than 1.5, the reason why they were picked to new screening in 96-deep-wells plate with more replicas of each clone to try to minimize the risk of selecting a false positive (Figure 3.11A).

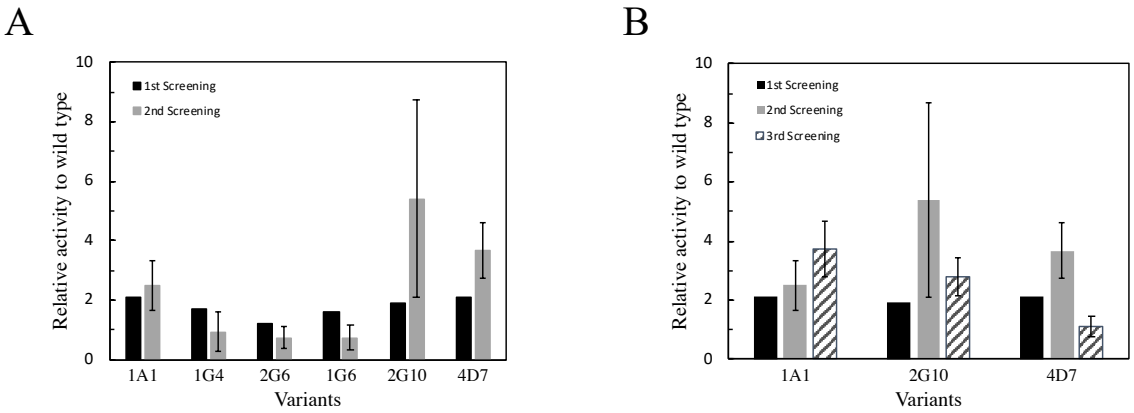

Figure 3.11 Activity relative to wild-type of each AsP2Ox variant picked to 96-wells plates during the first generation of directed evolution. In (A) is the data obtained in the 2nd screening for each of the six variants selected during the 1st screening (relative activity higher than 1.5). The black bars represent the relative activity obtained in the first screening (n=1) and the grey bars represent the relative activity obtained in the second screening (n=12). In (B) it is shown the data obtained for the three variants that had been selected in the 2nd screening (relative activity higher than 2.0). The black bars represent the relative activity obtained in the first screening (n=1), the grey bars represent the relative activity obtained in the second screening (n=12) and the dashed bars represent the relative activity obtained in the third rescreening (n= 24).

Finally, it was fixed a threshold of 2.0 for the relative activity which allowed to select three variants for a new rescreening **(**Figure 3.11B). In this last rescreening, 1A1 variant was the best hit variant reaching a relative activity of 3.7 ± 0.9 in comparison to wild-type, but 2G10 showed as well a good performance reaching a relative activity of 2.8 ± 0.6. An additional screening was performed by stretching liquid culture lines on a solid media plate (pre-supplemented with ampicillin and rhamnose). After growth of the cultures an 'Activity-on-plate' assay was performed (Figure 3.12). The results showed that 1A1 is better than the wild-type and 2G10, supporting the data from liquid screening and allowing to select with confidence variant 1A1 as the parent of the next generation of DE.

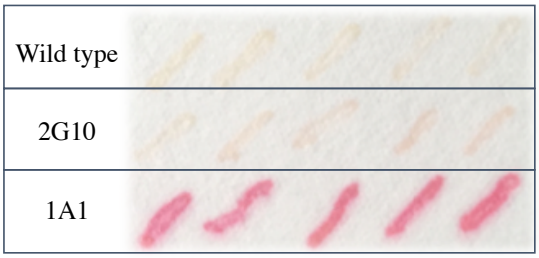

Figure 3.12 'Activity-on-plate' rescreening to compare activity of wild-type with 2G10 and 1A1 AsP2Ox variants. The principle applied was the similar to the one used in 'Activity-on-plate' assays. The disruption of the cells on the chromatographic paper was performed with 2 mg/mL of lysozyme and the reaction mixture contained 0.5 M of D-glucose, 8 U of HRP, 1 mM of AAP and 10 mM of DCHBS.

Both variants were sent to sequencing and the results revealed the introduction of one mutation in 1A1 variant replacing a glycine to a serine in position 366 and two mutations in variant 2G10 (Figure 3.13A) The structure analysis of the 1A1 variant using the AsP2Ox model showed that the amino acid residue 366 was located inside the substrate pocket and around ~10 Å to N5 of FAD (Figure 3.13B).

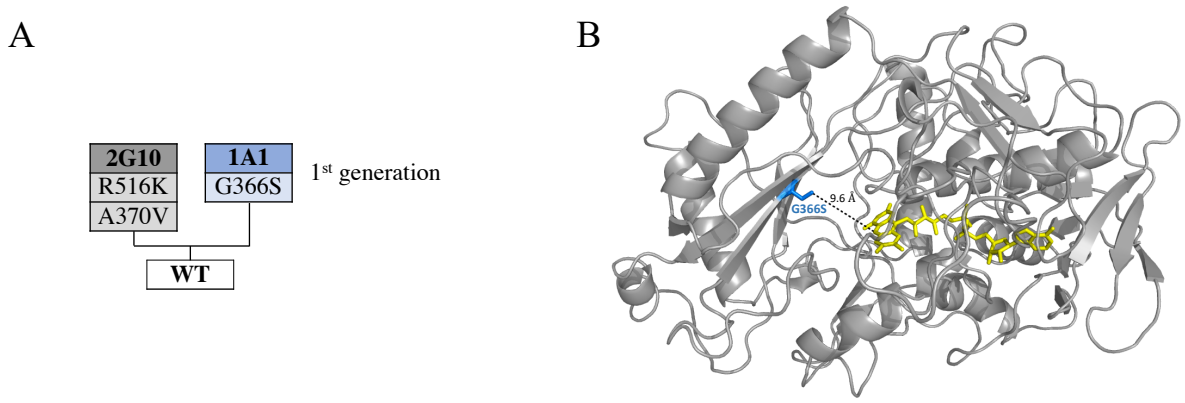

Figure 3.13 Summary of the first generation of directed evolution. (A) Evolution tree of AsP2Ox after the first generation, the 1A1 variant which carry a mutation in the position 366 from a glycine to a serine will be the parent of the second generation of directed evolution. (B) AsP2Ox model (based on *Trametes multicolour* structure) where it is possible to identify the mutation G366S (blue) located on the putatively substrate binding pocket, at ~10 Å of the N5 of FAD cofactor (yellow molecule).

3.2.3 Second generation of directed evolution

The 'Activity-on-plate' screening was performed using the 1A1 variant in order to validate the screening and showed that after disruption the majority of the cells did not display activity. Based on these results the disruption method was changed from disruption using lysozyme to a disruption with B-PER. However, since we have previously shown that some components in B-PER could act as AsP2Ox electron donor this screening could not accurately allow to distinguish improved variants for D-glucose and O_2 but only colonies that show the activity of interest, *i.e.* that are producing AsP2Ox.

In the liquid screenings, the CV using the 1A1 variant remains sufficiently low to allow identifying improved variants reason why the procedure was not modified.

In the second generation, ~4,000 colonies were screened, ~900 showed activity on the 'Activity-on-plate' and those were picked for 96-deep-wells plates.

In the first 96-wells plate screening using the 900 variants only 8 showed a relative activity 1.5-fold higher than the 1A1 parent (Figure 3.14A). A liquid rescreening was performed for those 8 variants and only the variant 5D5 showed improved activity (~3.3-fold higher than 1A1) (Figure 3.14B).

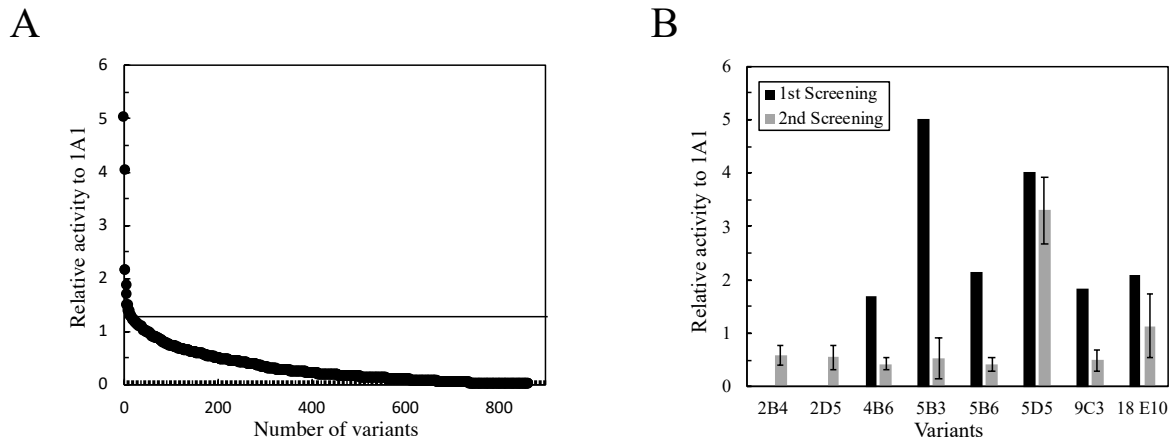

Figure 3.14 Activity relative to 1A1 obtained for each variant in 96-wells plate screening during the second generation of directed evolution. In (A) data displayed was obtained in the first screening for each of the ~900 variants selected during the 'Activity-on-plate' screening of 4,000 colonies screened, in (B) it is shown the data obtained for the eight variants that had been selected in the 1st screening (relative activity higher than 1.5). The black bars represent the relative activity obtained in the first screening (n=1), the grey bars represent the relative activity obtained in the second screening (n=12). For 2B4 and 2D5 the activity measured was not saved on the computer the reason why the bars from 1st rescreening are unavailable for these 2 variants.

To be confident about the improvement in this hit variant a final rescreening was performed in liquid media using both the 5D5 and 1A1 variants revealing that 5D5 had a relative activity of 5.0 ± 0.9 (Figure 3.15A).

The DNA sequence of variant 5D5 showed four mutations. One was silent mutation in the codon that codifies for serine in position 22, this mutation should not interfere in protein activity. However, it could hypothetically change protein production yields but the analysis of the codon usage in *E. coli* of the previous and the new codon revealed that both are typically used at the same ratio which suggest that protein production should not be affected by the insertion of this mutation.

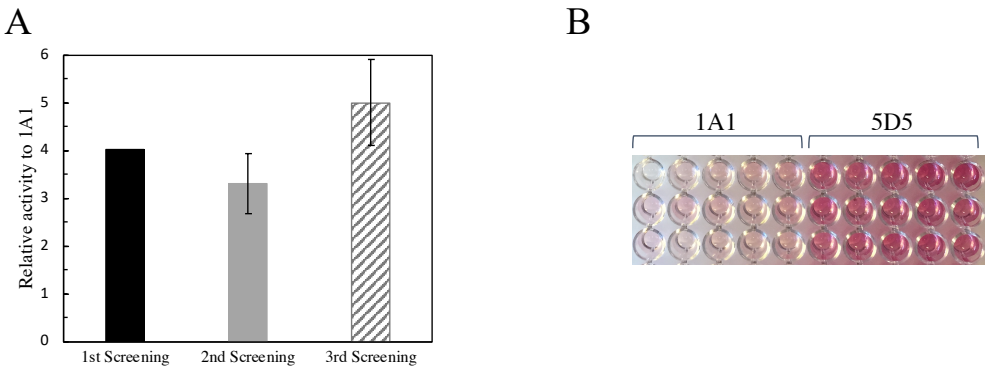

Figure 3.15 Final screening that support the selection of 5D5 as the hit variant of second generation.(A) Summary of activity relative to 1A1 for 5D5 variant during liquid medium screenings performed. The black bars represent the relative activity obtained for 5D5 in the first screening (n=1), the grey bars represent the relative activity obtained for 5D5 in the second screening (n=12) and the dashed bars represent the relative activity obtained in the third screening (n= 40). In (B) is displayed a picture of some wells of the plate performed for the 3rd screening where is visible the difference on activity between 1A1 (left) and 5D5 (right). The assay was performed in the presence of 0.1 M of D-glucose, 8 U of HRP, 1 mM of AAP and 10 mM of DCHBS at 25ºC.

Two mutations in 5D5 were a change from an alanine that is a hydrophobic amino acid to a threonine, a polar uncharged amino acid, and they occurred in the positions 75 and 206. The fourth mutation in 5D5 is a replacement of a glutamine to histidine in position 295 which represents a change from a polar uncharged to a (positive) charged amino acid (Figure 3.16A). The introduction of these mutations in the model structure shows that mutations A75T and A206T are at the surface and the Q295H is inside of the substrate binding pocket at ~11 Å to N5 of FAD cofactor (Figure 3.16B).

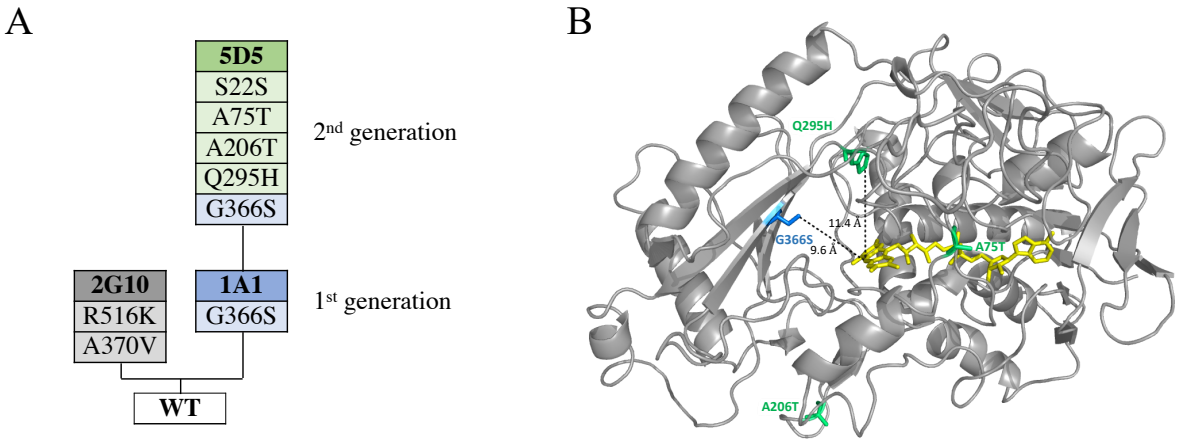

Figure 3.16 Summary of the second generation of directed evolution. (A) Evolution tree of AsP2Ox. The hit from the second generation, the 5D5 variant, carry one synonymous mutation in position 22, a mutation G366S that raised in the first generation and additionally three non-synonymous mutations (an alanine for a threonine in positions 75 and 206 and a glutamine to a histidine in the position 295. (B) AsP2Ox model (based on *Trametes multicolour* structure) where is possible to identify all mutations that are in 5D5 variant. In blue is the mutation introduced during the first generation and in green the mutations introduced during the second round of directed evolution (the identification of each mutation is on the figure). By the observation it can be conclude that the mutation A75T and A206T are in the surrounding of the substrate pocket (at ~17 Å and ~21 Å, respectively, from the N5 of FAD cofactor) and the mutation Q295H is inside of the putatively substrate binding pocket at ~11 Å of the N5 of FAD cofactor (yellow molecule) and at ~7 Å of G366S mutation.

3.3 Kinetic characterization of DE's hit variants

3.3.1 Protein production and pH profiles

After the evolution of AsP2Ox we have characterized thoroughly each purified variant in order to start establishing structure-function relationships and foster the knowledge on the biochemistry and range of application of P2Oxs.

The first general property analysed was the functional protein production of each variant (Table 3.6). During this thesis, the protein quantification was performed by quantifying the FAD cofactor because this would allow to consider the functional fraction of enzyme preparations that is usually different of total protein quantification. This is due to not only protein impurities, but also because some enzymes molecules did not incorporate properly or lose, for example, during purification, the FAD co-factor. The results show that the 1A1 variant, from the first generation, have 2-fold higher proportion of functional protein when compared with wild-type which could be a factor that contributed for the higher relative activity verified during the 96-wells plate screening assays. The 5D5 variant, from the second generation, shows a total protein production higher than the 1A1 variant, however, the standard deviation between the batches is high (around 25%) which does not allow to be confident about the production yields improvement.

Table 3.6 AsP2Ox protein production yields and optimal pH for the directed evolution hit variants. Total protein yield production was measured by Bradford method and also by Abs_{280nm} after purification of each enzyme and was quantified in relation to the volume used for cell growth. The functional AsP2Ox production yield was determined by FAD concentration (absorbance at 450 nm) and it was quantified in relation to the volume used for cell growth. The optimal pH for each variant was achieved by determining the maximum activity in a range of pH values (pH profile of purified enzyme).

Variant	Mutations	Production of AsP2Ox (Total) (mg $L_{culture}^{-1}$)		Production of functional AsP2Ox (mg $L_{culture}^{-1}$)	Optimum pH
		Bradford	Abs_{280nm}		
Wild-type	-	21.3 ± 5.9	14.1 ± 4.8	6.7 ± 1.4	7.5
1A1	G366S	39.2 ± 5.3	28.9 ± 3.2	14.0 ± 1.3	7.5
5D5	S22S A75T A206T Q295H G366S	85.0 ± 31.8	48.1 ± 4.4	20.4 ± 5.1	8.5

The pH profile was determined for each variant (Figure 3.17), and variant 1A1 shows the same value of optimal pH as the wild-type while the variant 5D5 has a pH optimal shifted 1 unit towards alkaline range (Table 3.6).

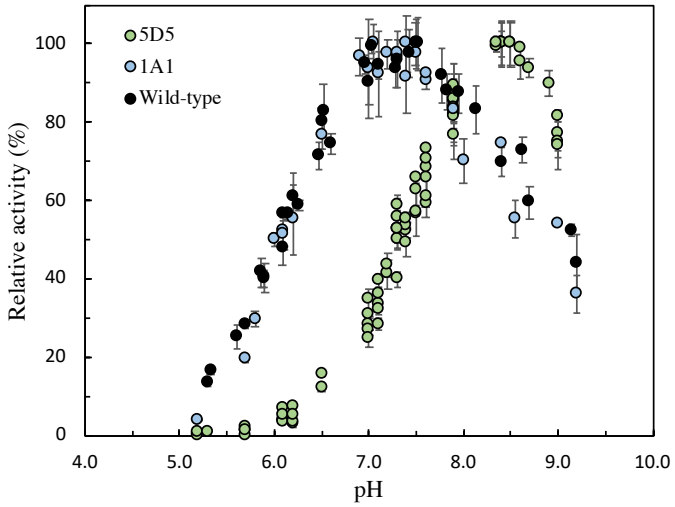

Figure 3.17 pH profile of wild-type, 1A1 and 5D5 AsP2Ox variants. The detection method used was HRP-AAP/DCHBS coupled assay. The data suggest that the optimal pH for wild-type (black circles) and 1A1 (blue circles) is between 7.0 and 7.5. For 5D5 variant (green circles) the optimal pH is 8.5. All assays were performed in presence of 0.3 M of D-glucose at 37ºC and the buffer used was Briton and Robinson (pH range 5 to 9). The pH of the reactional mixture was verified using a pH electrode. The relative activity was calculated considering the maximum of activity (optimal pH) as 100 %.

3.3.2 Transient state kinetic analysis of wild-type and variants

A transient state analysis was performed using the stopped-flow apparatus in order to get insights on the catalytic mechanism of AsP2Ox. In this analysis, the changes of absorbance at 460 nm following directly the FAD cofactor of the enzyme was monitored (Figure 3.18). Some traces obtained on stopped-flow experiments are shown in Figure 3.19.

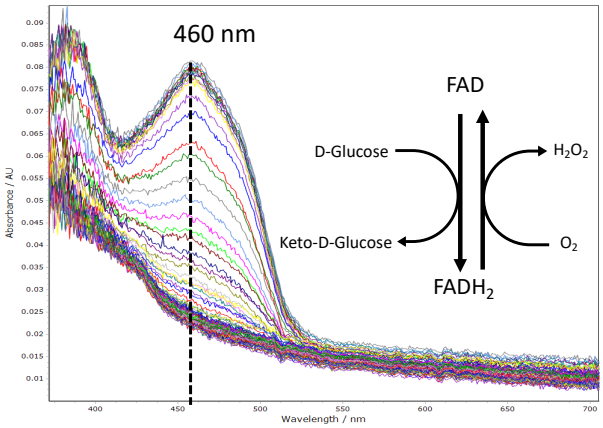

Figure 3.18 Time-course spectra set for one shoot in stopped flow apparatus. The raw data set (spectra) shows an assay for transient state kinetics where it is possible to follow the changes of absorbance at 460 nm. The scheme represented shows that when FAD is reduced to $FADH_2$ by D-glucose leads to a decrease of the signal at 460 nm and when the $FADH_2$ is oxidized by O_2 to FAD the 460 nm signal increases.

The first experiments were performed with the wild-type AsP2Ox for both half-reactions (reductive and oxidative) in order to elucidate the limiting step of the catalytic cycle.

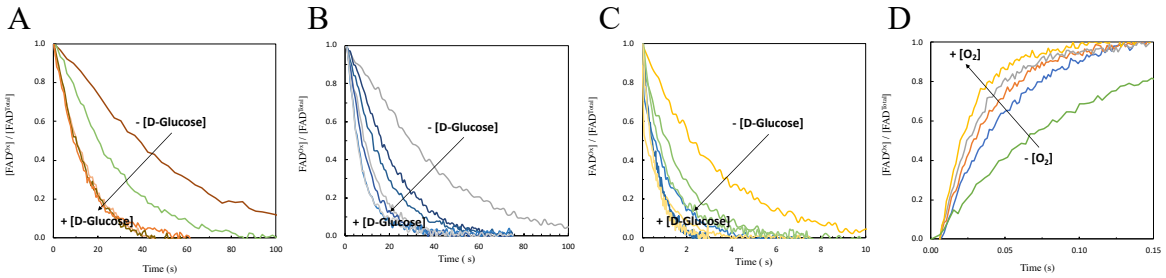

Figure 3.19 Transient-state analysis of the different variants of AsP2Ox (Traces). Some traces (raw data) obtained in transient state analysis for reductive half reaction of (A) wild-type, (B) 1A1 variant and (C) 5D5 variant changing the D-glucose concentration and for (D) oxidative half reaction of the wild-type changing the dioxygen concentration. For assays with wild-type and 1A1 variant the buffer used was the 100 mM sodium phosphates pH 7.5 and for assays with 5D5 variant it was used 50 mM Tris-HCl pH 8.5.

The analysis of the results (Figure 3.20) showed that the second-order constant for the reductive half-reaction in wild-type is k_{red}^{wt} = 0.13 ± 0.04 M^{-1} s^{-1} and for the oxidative half-reaction the value is k_{ox}^{wt} = (7.5 ± 0.6) × 10^5 M^{-1} s^{-1}.The k_{ox}^{wt} is 6 orders of magnitude higher than the k_{red}^{wt} clearly showing that the reductive half-reaction (the oxidation step of D-glucose to keto-D-glucose) is the limiting step of the overall reaction. This result suggests that increasing the enzyme reactivity for D-glucose is clearly key to improve the overall efficiency of AsP2Ox enzyme.

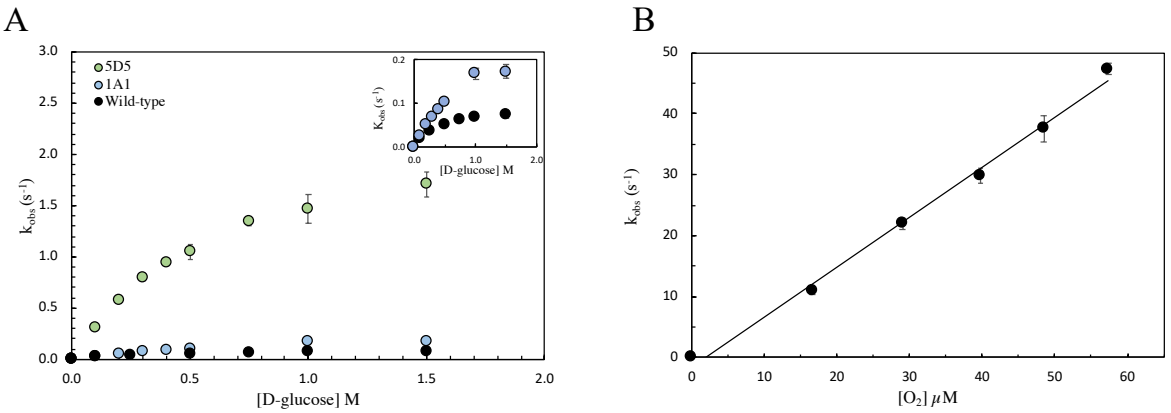

Figure 3.20 Transient steady-state analysis of AsP2Ox enzyme variants. (A) kinetics of the reductive-half reaction of the directed evolution variants of AsP2Ox determined by adding D-glucose and following the decrease of absorbance at 460 nm during time (in stopped-flow apparatus). The black circles represent the data obtained for wild-type (the slope of the linear regression of the four points allow to determine the second order constant for reductive half-reaction k_{red}^{wt} = 0.13 ± 0.04 M^{-1} s^{-1}), the blue circles represent the data obtained for 1A1 variant (the slope of the linear regression of the first five points allow to determine the second order constant for reductive half-reaction k_{red}^{1A1} = 0.23 ± 0.02 M^{-1} s^{-1}) and the green circles represent the data obtained for 5D5 variant (the slope of the linear regression of the first five points allow to determine the second order constant for reductive half-reaction k_{red}^{5d5} = 2.6 ± 0.4 M^{-1} s^{-1}). (B) Kinetic obtained for the oxidative half-reaction for the wild-type (the slope of the linear regression of data allow to determine the second order constant for oxidative half-reaction k_{ox}^{wt} = (7.5 ± 0.6) × 10^5 M^{-1} s^{-1}). All data were obtained at 25ºC.

Next, the transient state analysis of the reductive half-reaction was performed for 1A1 and 5D5 variants (Figure 3.20A). The second-order constants for reductive half-reaction for 1A1 (k_{red}^{1A1} = 0.23 ± 0.02 M^{-1} s^{-1}) and 5D5 (k_{red}^{5d5} = 2.6 ± 0.4 M^{-1} s^{-1}) variants are 2- and 20-fold higher, respectively, as compared to wild-type. These results suggest, that the protein evolved for D-glucose oxidation during the directed evolution process.

3.3.3 Steady-state kinetic parameters for D-glucose

To compare the overall reaction performed by AsP2Ox and also to determine the apparent steady-state kinetic parameters the steady-state assays for each variant using D-glucose and O_2 as substrates and the HRP-AAP/DCHBS coupled assay. The summary of the parameters is in Table 3.7 and kinetics curves can be observed in Figure 3.21.

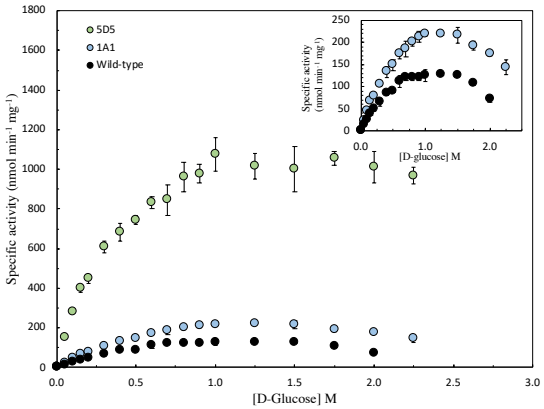

Figure 3.21 Steady-state kinetic curves for the variants of AsP2Ox. Example of steady-state kinetics obtained using the HRP-AAP/DCHBS method of detection for wild-type (black circles), 1A1 (blue circles) and 5D5 (black circles). The assays were performed at 37ºC and the reaction mix contains 0.1 mM of AAP, 1 mM of DCHBS and 8 U of HRP in 100 mM sodium phosphates buffer pH 7.5 (for wild-type and 1A1 variant) or in 50 mM Tris-HCl pH 8.5 (for 5D5 variant).

Table 3.7 Apparent steady-state kinetic parameters of wild-type , 1A1 and 5D5 AsP2Ox variants using D-glucose as electron donor and O_2 as electron acceptor. The data was obtained using the HRP-AAP/DCHBS coupled assay at 37ºC in 100 mM sodium phosphate buffer at pH 7.5 (for wild-type and 1A1) or in 50 mM Tris-HCl pH 8.5 (for 5D5 variant). The routine reaction mixture contained 0.1 mM of AAP, 1 mM of DCHBS and 8 U of HRP. The kinetic parameters were determined by OriginLab by fitting the data directly on the Michaelis-Menten equation.

Variant	K_m (M)	k_{cat} (s^{-1})	k_{cat}/K_m (M^{-1} s^{-1})
Wild-type	0.37 ± 0.13	0.18 ± 0.01	0.51 ± 0.10
1A1	0.54 ± 0.11	0.36 ± 0.08	0.67 ± 0.08
5D5	0.33 ± 0.05	1.00 ± 0.22	3.22 ± 0.39

The results show that the K_m increases slightly in the 1A1 variant but in 5D5 decreases back to a value closer to those obtained in the wild-type enzyme. The k_{cat} increased 2-fold during the evolution in the first generation and 6-fold in the second generation when wild-type is used as a reference. These changes on the k_{cat} influence the catalytic efficiency, k_{cat}/K_m, that increases during evolution reaching the value 3.22 ± 0.39 M^{-1} s^{-1} for 5D5 variant (which is 6-fold higher than wild-type).
The steady-state data shows that k_{cat} was the parameter more affected during the evolution of the protein. The comparison of second-order constants for the reductive half-reaction obtained in transient state with the k_{cat}/K_m obtained in the steady-state assays revealed that the values are in the same order of magnitude; the observed differences can be related to differences in temperature since in steady-state assays the temperature was used was of 37ºC (the optimal temperature for protein activity) and in transient-state assays it was used 25ºC.

3.3.4 Steady-state kinetic parameters for dioxygen

A steady-state analysis was also performed by following directly the oxygen consumption in an Oxygraph® device. In this approach, the concentration of D-glucose was fixed to 1 M in all assays to ensure substrate saturation. Dioxygen concentration was varied in the reaction mixture. The steady-state parameters obtained are summarized in Table 3.8.

Table 3.8 Apparent steady-state kinetic parameters obtained by following the O_2 consumption for wild-type, 1A1 and 5D5 AsP2Ox variants (using the Oxygraph®). The data was obtained at 37ºC in 100 mM sodium phosphate buffer at pH 7.5 (for wild-type and 1A1) or in 50 mM Tris-HCl buffer at pH 8.5 in the presence of 1 M of D-glucose as sugar substrate. For wild-type and 1A1 the kinetic parameters were obtained using the OriginLab by fitting the data directly into the Michaelis-Menten equation. For the 5D5 variant the catalytic efficiency was determined by the approximation [S] << K_m on the Michaelis-Menten equation.

Variant	K_m (M)	k_{cat} (s^{-1})	k_{cat}/K_m (M^{-1} s^{-1})
Wild type	$(171.9 \pm 50.9) \times 10^{-6}$	0.06	355.9
1A1	$(174.7 \pm 74.1) \times 10^{-6}$	0.12	686.9
5D5	-	-	3600.0

For wild-type and 1A1 variant the kinetics obtained followed Michaelis-Menten allowing to determine all apparent steady-state parameters while for 5D5 the kinetics obtained was linear which just allowed to determine the catalytic efficiency for O_2 (using the approximation [S]<<K_m) (Figure S6.4).
The K_m for O_2 in wild-type and in 1A1 are similar which means that the O_2 affinity did not change. The k_{cat} of 1A1 is 2-fold higher than the wild-type which is consistent with the ratio obtained in the kinetics performed by varying D-glucose concentration in the coupled assay reaction (Table 3.7). Even the kinetic parameters are in the same magnitude order, the values are 3-fold lower when the k_{cat} following the O_2 consumption is compared with k_{cat} obtained in steady-state assays using the coupled assay which is not expected since k_{cat} reflects the number of catalytic cycles per time unit which should be independent of the measuring method. Finally, the catalytic efficiency for O_2 increased during the evolution process improving around 10-fold in 5D5variant as compared with wild-type.

3.4 Effect mutations introduced during DE

During the evolution of a protein by DE is not mandatory to know the role of each mutation introduced during the generations, although all information that we can get represents a plus to understand the system that we are working with.
During the first generation, only one mutation was introduced by the epPCR which makes easy the correlation of the genotype with the phenotype but in the second generation, three non-synonymous mutations were introduced which impairs the identification of those that are crucial for the activity improvement.
To try to understand the role of each mutation introduced in the 2nd generation of DE, site-directed mutagenesis was performed to introduce each mutation on the wild-type protein leading the formation of the single mutants A75T, A206T, and Q295H. The pH profile (Figure 3.22), protein production yields and steady-state kinetics using HRP-AAP/DCHBS coupled assay were performed for each mutant and the parameters obtained are summarized in Table 3.9. Some kinetic curves are displayed in Figure S6.5.

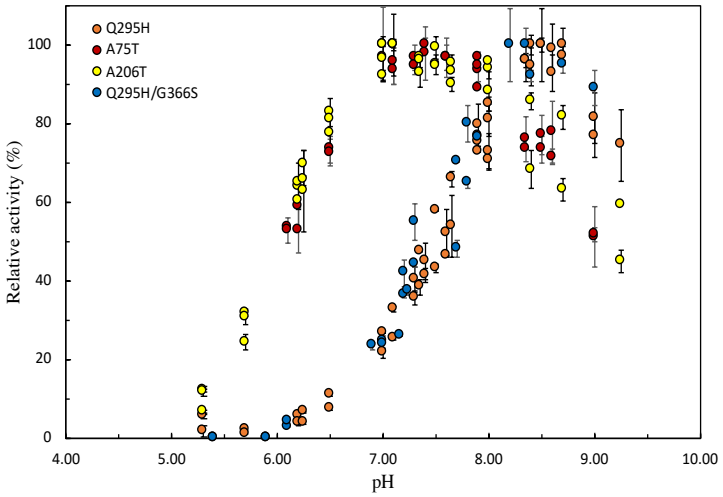

Figure 3.22 pH profile of AsP2Ox single mutants A75T, A206T and Q295H and for double mutant Q295H/G366S. The detection method used was HRP-AAP/DCHBS coupled assay. The data suggest that the optimal pH for A75T (red circles) and A206T (yellow circles) is between 7.0 and 7.5. For Q295H (orange circles) and Q295H/G366S (blue circles) mutants the optimal pH is 8.5. All assays were performed in presence of 0.3 M of D-glucose at 37ºC and the buffer used was Briton and Robinson (pH range 5 to 9). The pH of the reactional mixture was verified using a pH electrode. The relative activity was calculated considering the maximum of activity (at optimal pH) as 100 %.

The results of the pH profile allow to conclude that the mutation responsible by the optimal pH shift in 5D5 is the Q295H because the single mutant Q295H showed the same shift which should be related to the side chain of the histidine.

Table 3.9 Apparent steady-state kinetic parameters (for D-glucose and O_2), protein yields production and optimal pH of the AsP2Ox mutants A75T, A206T, Q295H and Q295H/G366S. Total protein yield production was measured by Bradford method and also by Abs_{280nm} after purification of each enzyme and was quantified in relation to the volume used for cell growth. The functional AsP2Ox production yield was determined by FAD concentration (absorbance at 450 nm) and it was quantified in relation to the volume used for cell growth. The optimal pH for each variant was achieved by determining the maximum activity in a range of pH values (pH profile of purified enzyme). Steady-state kinetic parameters were obtained using HRP-AAP/DCHBS coupled assay at 37ºC in 100 mM sodium phosphate buffer at pH 7.5 (for wild-type, A75T and A206T mutants) or in 50 mM Tris-HCl pH 8.5 (for 5D5, Q295H or Q295H/G366S mutants). The routine reaction mixture contained 0.1 mM of AAP, 1 mM of DCHBS and 8 U of HRP. The kinetic parameters were determined by OriginLab by fitting the data directly on the Michaelis-Menten equation. ND means not determined.

Variant/ Mutant	Production of (total) AsP2Ox (mg $L_{culture}^{-1}$)		Production of functional AsP2Ox (mg $L_{culture}^{-1}$)	Optimum pH	K_m (M)	k_{cat} (s^{-1})	k_{cat}/K_m (M^{-1} s^{-1})
	Bradford	Abs_{280nm}					
Wild-type	21.3 ± 5.9	14.1 ± 4.8	6.7 ± 1.4	7.5	0.37 ± 0.13	0.18 ± 0.01	0.51 ± 0.10
5D5	85.0 ± 31.8	48.1 ± 4.4	20.4 ± 5.1	8.5	0.33 ± 0.05	1.00 ± 0.22	3.22 ± 0.39
A75T	9.3 ± ND	16.2 ± ND	7.2 ± ND	7.5	0.59 ± 0.14	0.21 ± 0.03	0.37 ± 0.05
A206T	28.2 ± ND	33.0 ± ND	12.0 ± ND	7.5	0.56 ± 0.05	0.29 ± 0.03	0.52 ± 0.01
Q295H	11.7 ± ND	16.3 ± ND	8.5 ± ND	8.5	0.28 ± 0.02	0.51 ± 0.02	1.84 ± 0.06
Q295H/G366S	42.8 ± ND	18.7 ± ND	12.3 ± ND	8.5	0.28 ± 0.02	0.89 ± 0.03	3.22 ± 0.34

The kinetic parameters of both A75T and A206T variants are similar to wild-type and lower than variant 5D5 showing that these mutations located at the surface far away (respectively, at ~17 Å and ~21 Å from N5 of FAD co-factor) from the active site, have an apparent neutral character in what regards the activity using D-glucose and O_2. The single variant Q295H shows a K_m close to those exhibited by 5D5 and a k_{cat} and k_{cat}/K_m s ~2.5-fold when compared with wild-type and around half of those exhibited by 5D5.

Consequently, the values of k_{cat} and k_{cat}/K_m in the single mutant Q295H, located at the substrate pocket at ~11 Å distance of N5 of FAD cofactor (Figure 3.16), suggest that this mutation has an important beneficial role in the catalytic enhancement of 5D5 variant. However, the mutation Q295H alone did not reach the values obtained in 5D5 which suggest that other(s) mutation(s) present in this hit variant should cooperate with the mutation Q295H to improve the activity. The only way to check for this apparent cooperation is to perform all possible double and triple mutants and calculate the apparent steady-state parameters. The analysis of mutations that were introduced during the evolution in the model structure shows that mutation G366S (inserted in the first generation) is located on the substrate pocket similarly to mutation Q295H (the distance between them is ~7 Å) which makes the cooperation between the two mutations a hypothetical possibility.

To test the synergy of G366S and Q295H mutations the double mutant Q295H/G366S was constructed. This double mutant showed an optimal pH of 8.5 (Figure 3.22) and the steady-state kinetics using HRP-AAP/DCHBS coupled assay (Table 3.9) showed that catalytic efficiency is 3.22 ± 0.34 M^{-1} s^{-1} which is the same value obtained for 5D5.

These results suggest that both Q295H and G366S are important mutations for the improvement of AsP2Ox activity and that they display an epistatic effect since the effect of mutations together is higher than the effect of each mutation individually. In addition, the double mutant Q295H/G366S did not reach the functional protein production yields obtained for 5D5 (Table 3.9) which suggest that the mutations A75T and A206T in that variant can be related with higher yields of AsP2Ox production.

4. Conclusions

This work is part of a project which main goal is the improvement of the first characterized bacterial P2Ox using directed evolution techniques to originate variants with improved kinetics for D-glucose to be applied as first-generation biosensors for glycemia monitoring.

The development and optimization of an efficient and reliable high throughput screenings methodologies, during this work, allowed the analysis of some several thousands of variants in two rounds of directed. The 'Activity-on-plate', a qualitative colorimetric assay, showed to be a useful tool to select variants for a subsequent 96-wells plate screening. This last, a quantitative approach, which was optimized and validated for the growth of recombinant *E. coli* and cells disruption. At the end of each directed evolution round, a hit variant was successfully achieved (1A1 and 5D5, in the first- and second-generation, respectively) showing improved properties when compared with its parent enzyme; using crude extracts, 1A1 activity relative to wild-type was ~4-fold higher and 5D5 activity relative to 1A1 was ~5-fold higher.

Enzyme purification and characterization of the obtained variants revealed that in the first-generation variant 1A1, harboring the mutation G366S, located at the substrate binding pocket, was produced at higher yields and showed a k_{cat} value ~2-fold higher as compared with wild-type. In the second generation, 5D5 variant, that inserted additional non-synonymous mutations Q295H, A206T and A75T, shows an alkaline pH optimal shifted to 8.5 and the k_{cat} constant had an improvement of ~6-fold higher than the wild-type enzyme resulting in an enzyme with higher catalytic efficiency. Single and double mutants constructed using SDM and its kinetic analysis had shown that mutation Q295H was the responsible for the alkaline pH shift obtained. The Q295H and G366S mutations (~7 Å from each other) interact synergistically and have a direct role in the improvement of the catalytic efficiency obtained for D-glucose using O_2 as electron acceptor. The other two mutations inserted A75T and A206T, did not show any apparent role in the kinetic improvement detected but they can be involved in the "upgrade" of other enzymatic properties, for example, protein stability or solubility resulting in the higher functional protein production yields exhibited in 5D5 variant. The kinetics of oxygen consumption suggest a high K_m of 5D5 for dioxygen (considering the standard concentrations of this gas in solutions), although the catalytic efficiency showed a 10-fold increase.

The transient-state kinetics of wild-type, showed that the reductive half-reaction (corresponding to step of reduction of enzyme FAD co-factor to $FADH_2$) is the rate limiting step of the overall reaction and, allowed to confirmed the increase of the second-order constant for that half-reaction during evolution in the 5D5 variant.

The advances obtained in AsP2Ox evolution, during this work, were notable, however the needed kinetic values that would allow the application of this enzyme in biosensors for monitoring glycemia were still not achieved. This is mainly due to the fact that 5D5 variant remains with a very high K_m for D-glucose (in the order of molar) while typical GOxs have a K_m in the order of millimolar [77], [78] which means that more work is needed towards that goal. Additionally, the majority of GOxs have a k_{cat} 1-2 orders of magnitude higher than those obtained for 5D5 [78]. These conclusions motivate the MET group to continue the AsP2Ox evolution to decrease K_m parameter and to also increase the k_{cat} that it can be applied in the desired application.

5. References

[1] A. N. Reshetilov, P. V. Iliasov, and T. A. Reshetilova, "The microbial cell based biosensors," in *Intechopen*, intechopen, 2010.

[2] H. H. Nguyen, S. H. Lee, U. J. Lee, C. D. Fermin, and M. Kim, "Immobilized enzymes in biosensor applications," *Materials (Basel).*, vol. 12, no. 1, pp. 1–34, 2019.

[3] S. Ferri, K. Kojima, and K. Sode, "Review of Glucose Oxidases and Glucose Dehydrogenases : A bird's eye view of glucose sensing enzymes," vol. 5, no. 5, pp. 1068–1076, 2011.

[4] F. Giffhorn, "Fungal pyranose oxidases: Occurrence, properties and biotechnical applications in carbohydrate chemistry," *Appl. Microbiol. Biotechnol.*, vol. 54, no. 6, pp. 727–740, 2000.

[5] M. J. Artolozaga, E. Kubátová, J. Volc, and H. M. Kalisz, "Pyranose 2-oxidase from Phanerochaete chrysosporium - Further biochemical characterisation," *Appl. Microbiol. Biotechnol.*, vol. 47, no. 5, pp. 508–514, 1997.

[6] F. Jing *et al.*, "A novel fully enzymatic method for determining glucose and 1,5-anhydro-d-glucitol in serum of one cuvette," *Appl. Biochem. Biotechnol.*, vol. 150, no. 3, pp. 327–335, 2008.

[7] Y. F. et Al, "Fully Enzymatic for Determining 1 ,5-Anhydro-D-glucitol in Serum," vol. 40, no. 11, pp. 2013–2016, 1994.

[8] K. M. Dungan, "1,5-Anhydroglucitol (GlycoMark^{TM}) as a marker of short-term glycemic control and glycemic excursions," *Expert Rev. Mol. Diagn.*, vol. 8, no. 1, pp. 9–19, 2008.

[9] B. Martin Hallberg, C. Leitner, D. Haltrich, and C. Divne, "Crystal structure of the 270 kDa homotetrameric lignin-degrading enzyme pyranose 2-oxidase," *J. Mol. Biol.*, vol. 341, no. 3, pp. 781–796, 2004.

[10] T. Wongnate and P. Chaiyen, "The substrate oxidation mechanism of pyranose 2-oxidase and other related enzymes in the glucose-methanol-choline superfamily," *FEBS J.*, vol. 280, no. 13, pp. 3009–3027, 2013.

[11] P. Macheroux, "UV-Visible Spectroscopy as a Tool to Study Flavoproteins," in *Flavoprotein protocols*, Chapman, S., vol. 131, Humana Press.

[12] T. P. Begley and W. J. H. van Berkel, "Flavoenzymes, Chemistry of," *Wiley Encycl. Chem. Biol.*, no. January 2008, 2008.

[13] Y. Takakura and S. Kuwata, "Purification, Characterization, and Molecular Cloning of a Pyranose Oxidase from the Fruit Body of the Basidiomycete, Tricholoma matsutake," *Biosci. Biotechnol. Biochem.*, vol. 67, no. 12, pp. 2598–2607, 2003.

[14] A. Huwig, H. J. Danneel, and F. Giffhorn, "Laboratory procedures for producing 2-keto-d-glucose, 2-keto-d-xylose and 5-keto-d-fructose from d-glucose, d-xylose and l-sorbose with immobilized pyranose oxidase of Peniophora gigantea," *J. Biotechnol.*, vol. 32, no. 3, pp. 309–315, 1994.

[15] P. Halada, C. Leitner, P. Sedmera, D. Haltrich, and J. Volc, "Identification of the covalent flavin adenine dinucleotide-binding region in pyranose 2-oxidase from Trametes multicolor," *Anal. Biochem.*, vol. 314, no. 2, pp. 235–242, 2003.

[16] S. Freimund, A. Huwig, F. Giffhorn, and S. Köpper, "Rare keto-aldoses from enzymatic oxidation: Substrates and oxidation products of pyranose 2-oxidase," *Chem. - A Eur. J.*, vol. 4, no. 12, pp. 2442–2455, 1998.

[17] M. Kujawa *et al.*, "Structural basis for substrate binding and regioselective oxidation of monosaccharides at C3 by pyranose 2-oxidase," *J. Biol. Chem.*, vol. 281, no. 46, pp. 35104–35115, 2006.

[18] T. C. Tan, D. Haltrich, and C. Divne, "Regioselective control of β-d-glucose oxidation by pyranose 2-oxidase is intimately coupled to conformational degeneracy," *J. Mol. Biol.*, vol. 409, no. 4, pp. 588–600, 2011.

[19] I. Pisanelli *et al.*, "Pyranose 2-oxidase from Phanerochaete chrysosporium-Expression in E. coli and biochemical characterization," *J. Biotechnol.*, vol. 142, no. 2, pp. 97–106, 2009.

[20] C. Salaheddin *et al.*, "Characterisation of recombinant pyranose oxidase from the cultivated mycorrhizal basidiomycete Lyophyllum shimeji (hon-shimeji)," *Microb. Cell Fact.*, vol. 9, pp. 1–12, 2010.

[21] J. Sucharitakul, M. Prongjit, D. Haltrich, and P. Chaiyen, "Detection of a C4a-hydroperoxyflavin intermediate in the reaction of a flavoprotein oxidase," *Biochemistry*, vol. 47, no. 33, pp. 8485–8490, 2008.

[22] F. Giffhorn, S. Ko, A. Huwig, and S. Freimund, "Rare sugars and sugar-based synthons by chemo-enzymatic synthesis," vol. 27, pp. 734–742, 2000.

[23] S. Freimund and S. Köpper, "The composition of 2-keto aldoses in organic solvents as determined by NMR spectroscopy," *Carbohydr. Res.*, vol. 339, no. 2, pp. 217–220, 2004.

[24] S. Mendes *et al.*, "Characterization of a bacterial pyranose 2-oxidase from Arthrobacter siccitolerans," *J. Mol. Catal. B Enzym.*, vol. 133, pp. S34–S43, 2016.

[25] H. J. Danneel, M. Ullrich, and F. Giffhorn, "Goal-oriented screening method for carbohydrate oxidases produced by filamentous fungi," *Enzyme Microb. Technol.*, vol. 14, no. 11, pp. 898–903, 1992.

[26] M. Prongjit, J. Sucharitakul, T. Wongnate, D. Haltrich, and P. Chaiyen, "Kinetic mechanism of pyranose 2-oxidase from Trametes multicolor," *Biochemistry*, vol. 48, no. 19, pp. 4170–4180, 2009.

[27] F. W. Janssen and H. W. Ruelius, "Pyranose Oxidase from Polyporus obtusus," in *Methods in Enzymology*, vol. 41, no. C, 1975, pp. 170–173.

[28] P. L. Herzog *et al.*, "Versatile oxidase and dehydrogenase activities of bacterial pyranose 2-oxidase facilitate redox cycling with manganese peroxidase in vitro," *Appl. Environ. Microbiol.*, vol. 85, no. 13, pp. 1–15, 2019.

[29] G. Daniel, J. Volc, E. Kubatova, and T. Nilsson, "Ultrastructural and immunocytochemical studies on the H2O2-producing enzyme pyranose oxidase in Phanerochaete chrysosporium grown under liquid culture conditions," *Appl. Environ. Microbiol.*, vol. 58, no. 11, pp. 3667–3676, 1992.

[30] I. Nishimura, K. Okada, and Y. Koyama, "Cloning and expression of pyranose oxidase cDNA from Coriolus versicolor in Escherichia coli," *J. Biotechnol.*, vol. 52, no. 1, pp. 11–20, 1996.

[31] G. Daniel, J. Volc, and E. Kubatova, "Pyranose oxidase, a major source of H2O2 during wood degradation by Phanerochaete chrysosporium, trametes versicolor, and Oudemansiella mucida," *Appl. Environ. Microbiol.*, vol. 60, no. 7, pp. 2524–2532, 1994.

[32] V. Lombard, H. Golaconda Ramulu, E. Drula, P. M. Coutinho, and B. Henrissat, "The carbohydrate-active enzymes database (CAZy) in 2013," *Nucleic Acids Res.*, vol. 42, no. D1, pp. 490–495, 2014.

[33] Y. Takakura, "*Tricholoma matsutake* fruit bodies secrete hydrogen peroxide as a potent inhibitor of fungal growth," *Can. J. Microbiol.*, vol. 61, no. 6, pp. 447–450, 2015.

[34] D. Kracher *et al.*, "Extracellular electron transfer systems fuel cellulose oxidative degradation," *Science (80-.).*, vol. 352, no. 6289, pp. 1098–1101, 2016.

[35] J. Volc, E. Kubfitovfi, P. Sedmera, G. Daniel, and J. Gabriel, "by the basidiomycete Phanerochaete chrysosporium," pp. 297–301, 1991.

[36] R. Baute, M. A. Baute, and G. Deffieux, "Proposed pathway to the pyrones cortalcerone and microthecin in fungi," *Phytochemistry*, vol. 26, no. 5, pp. 1395–1397, 1987.

[37] M. Bannwarth, S. Bastian, D. Heckmann-Pohl, F. Giffhorn, and G. E. Schulz, "Crystal structure of pyranose 2-oxidase from the white-rot fungus Peniophora sp.," *Biochemistry*, vol. 43, no. 37, pp. 11683–11690, 2004.

[38] N. Hassan *et al.*, "Crystal structures of Phanerochaete chrysosporium pyranose 2-oxidase suggest that the N-terminus acts as a propeptide that assists in homotetramer assembly," *FEBS Open Bio*, vol. 3, pp. 496–504, 2013.

[39] T. Wongnate, P. Surawatanawong, L. Chuaboon, N. Lawan, and P. Chaiyen, "The Mechanism of Sugar C−H Bond Oxidation by a Flavoprotein Oxidase Occurs by a Hydride Transfer Before Proton Abstraction," *Chem. - A Eur. J.*, vol. 25, no. 17, pp. 4460–4471, 2019.

[40] H. J. Busse, "Review of the taxonomy of the genus Arthrobacter, emendation of the genus arthrobacter sensu lato, proposal to reclassify selected species of the genus Arthrobacter in the novel genera Glutamicibacter gen. Nov., Paeniglutamicibacter gen. nov., Pseudogluta," *Int. J. Syst. Evol. Microbiol.*, vol. 66, no. 1, pp. 9–37, 2016.

[41] K. Zhang *et al.*, "Identification and characterization of a novel bacterial pyranose 2-oxidase from the lignocellulolytic bacterium Pantoea ananatis Sd-1," *Biotechnol. Lett.*, vol. 40, no. 5, pp. 871–880, 2018.

[42] P. K. Robinson, "Enzymes: principles and biotechnological applications," *Essays Biochem.*, vol. 59, pp. 1–41, 2015.

[43] F. Giffhorn, S. Köpper, A. Huwig, and S. Freimund, "Rare sugars and sugar-based synthons by chemo-enzymatic synthesis," *Enzyme Microb. Technol.*, vol. 27, no. 10, pp. 734–742, 2000.

[44] S. Freimund, L. Baldes, A. Huwig, and F. Giffhorn, "Enzymatic synthesis of D-glucosone 6-phosphate (D-arabino-hexos-2-ulose 6-(dihydrogen phosphate)) and NMR analysis of its isomeric forms," *Carbohydr. Res.*, vol. 337, no. 17, pp. 1585–1587, 2002.

[45] K. Koths, R. Halenbeck, and M. Moreland, "Synthesis of the antibiotic cortalcerone from d-glucose using pyranose 2-oxidase and a novel fungal enzyme, aldos-2-ulose dehydratase," *Carbohydr. Res.*, vol. 232, no. 1, pp. 59–75, 1992.

[46] L. Chuaboon *et al.*, "One-Pot Bioconversion of l-Arabinose to l-Ribulose in an Enzymatic Cascade," *Angew. Chemie - Int. Ed.*, vol. 58, no. 8, pp. 2428–2432, 2019.

[47] W. Haltrich, D., Leitner, C., Neuhauser and J. Nidetzky, B., Kulbe, K. D., & Volc, "A Convenient Enzymatic Procedure for the Production of Aldose-Free D -Tagatose," *Ann. New York Acad. Sci.*, vol. 864, pp. 295–299, 1998.

[48] N. Plumeré, J. Henig, and W. H. Campbell, "Enzyme-catalyzed O 2 removal system for electrochemical analysis under ambient air: Application in an amperometric nitrate biosensor," *Anal. Chem.*, vol. 84, no. 5, pp. 2141–2146, 2012.

[49] D. Brugger, I. Krondorfer, C. Shelswell, B. Huber-Dittes, D. Haltrich, and C. K. Peterbauer, "Engineering pyranose 2-oxidase for modified oxygen reactivity," *PLoS One*, vol. 9, no. 10, 2014.

[50] S. Bastian, M. J. Rekowski, K. Witte, D. M. Heckmann-Pohl, and F. Giffhorn, "Engineering of pyranose 2-oxidase from Peniophora gigantea towards improved thermostability and catalytic efficiency," *Appl. Microbiol. Biotechnol.*, vol. 67, no. 5, pp. 654–663, 2005.

[51] O. Spadiut *et al.*, "Engineering of pyranose 2-oxidase: Improvement for biofuel cell and food applications through semi-rational protein design," *J. Biotechnol.*, vol. 139, no. 3, pp. 250–257, 2009.

[52] D. M. Heckmann-Pohl, S. Bastian, S. Altmeier, and I. Antes, "Improvement of the fungal enzyme pyranose 2-oxidase using protein engineering," *J. Biotechnol.*, vol. 124, no. 1, pp. 26–40, 2006.

[53] D. W. Watkins *et al.*, "Construction and in vivo assembly of a catalytically proficient and hyperthermostable de novo enzyme," *Nat. Commun.*, vol. 8, no. 1, pp. 1–9, 2017.

[54] H. Leemhuis, R. M. Kelly, and L. Dijkhuizen, "Directed evolution of enzymes: Library screening strategies," *IUBMB Life*, vol. 61, no. 3, pp. 222–228, 2009.

[55] M. D. Lane and B. Seelig, "Advances in the directed evolution of proteins," *Curr. Opin. Chem.*

Biol., vol. 22, pp. 129–136, 2014.
[56] B. Turanli-Yildiz, C. Alkim, and Z. Cakar, "Protein Engineering Methods and Applications," *Protein Eng.*, pp. 33–58, 2012.
[57] R. Chen, "Enzyme engineering: Rational redesign versus Directed evolution," vol. 19, no. 1, pp. 13–14, 2001.
[58] N. M. Antikainen and S. F. Martin, "Altering protein specificity: Techniques and applications," *Bioorganic Med. Chem.*, vol. 13, no. 8, pp. 2701–2716, 2005.
[59] A. E. Nixon and S. M. Firestine, "Rational and 'irrational' design of proteins and their use in biotechnology," *IUBMB Life*, vol. 49, no. 3, pp. 181–187, 2000.
[60] G. J. Williams, A. S. Nelson, and A. Berry, "Directed evolution of enzymes for biocatalysis and the life sciences," *Cell. Mol. Life Sci.*, vol. 61, no. 24, pp. 3034–3046, 2004.
[61] M. D. Hughes, D. A. Nagel, A. F. Santos, A. J. Sutherland, and A. V. Hine, "Removing the redundancy from randomised gene libraries," *J. Mol. Biol.*, vol. 331, no. 5, pp. 973–979, 2003.
[62] I. P. Petrounia and F. H. Arnold, "Designed evolution of enzymatic properties," *Curr. Opin. Biotechnol.*, vol. 11, no. 4, pp. 325–330, 2000.
[63] A. A. Volkov and F. H. Arnold, "Directed evolution of biocatalysts," *Curr. Opin. Chem. Biol.*, no. 3, pp. 54–59, 1999.
[64] M. S. Packer and D. R. Liu, "Methods for the directed evolution of proteins," *Nat. Rev. Genet.*, vol. 16, no. 7, pp. 379–394, 2015.
[65] H. Xiao, Z. Bao, and H. Zhao, "High throughput screening and selection methods for directed enzyme evolution High throughput screening and selection methods for directed enzyme evolution Departments of Chemistry and Bioengineering , Institute for Genomic Biology ," 2014.
[66] P. C. Cirino, K. M. Mayer, and D. Umeno, "Generating Mutant Libraries Using Error-Prone PCR," *Dir. Evol. Libr. Creat.*, vol. 231, no. 12, pp. 3–10.
[67] E. O. McCullum, B. A. R. William, J. Zhang, and J. C. Chaput, "Random Mutagenesis by Error-prone PCR," *Methods Mol. Biol.*, vol. 634, no. 7, 2010.
[68] J. D. Bloom, M. M. Meyer, P. Meinhold, C. R. Otey, D. MacMillan, and F. H. Arnold, "Evolving strategies for enzyme engineering," *Curr. Opin. Struct. Biol.*, vol. 15, no. 4, pp. 447–452, 2005.
[69] M. Kikuchi and S. Harayama, "DNA shuffling and family shuffling for in vitro gene evolution," *Methods Mol Biol*, vol. 182, no. 16, pp. 243–257, 2002.
[70] S. Brakmann, "Discovery of superior enzymes by directed molecular evolution," *ChemBioChem*, vol. 2, no. 12, pp. 865–871, 2001.
[71] G. Yang and S. G. Withers, "Ultrahigh-throughput FACS-based screening for directed enzyme evolution," *ChemBioChem*, vol. 10, no. 17, pp. 2704–2715, 2009.
[72] K. K. Yang, Z. Wu, and F. H. Arnold, "Machine-learning-guided directed evolution for protein engineering," *Nat. Methods*, vol. 16, no. 8, pp. 687–694, 2019.
[73] D. P. H. M. Heuts, D. B. Janssen, and M. W. Fraaije, "Changing the substrate specificity of a chitooligosaccharide oxidase from Fusarium graminearum by model-inspired site-directed mutagenesis," *FEBS Lett.*, vol. 581, no. 25, pp. 4905–4909, 2007.
[74] D. G. Gibson, L. Young, R. Y. Chuang, J. C. Venter, C. A. Hutchison, and H. O. Smith, "Enzymatic assembly of DNA molecules up to several hundred kilobases," *Nat. Methods*, vol. 6, no. 5, pp. 343–345, 2009.
[75] S. A. Sedov, N. G. Belogurova, S. Shipovskov, A. V. Levashov, and P. A. Levashov, "Lysis of Escherichia coli cells by lysozyme: Discrimination between adsorption and enzyme action," *Colloids Surfaces B Biointerfaces*, vol. 88, no. 1, pp. 131–133, 2011.
[76] B. H. Johnson and M. H. Hecht, "Recombinant proteins can be isolated from E.coli cells by repeated cycles of freezing and thawing," *Nat. Biotechnol.*, vol. 7, no. september, pp. 136–140, 1994.

[77] J. Singh and N. Verma, “Glucose oxidase from Aspergillus niger: Production, characterization and immobilization for glucose oxidation.,” *Adv. Appl. Sci. Res.*, vol. 4, no. 3, pp. 250–257, 2013.
[78] C. Momeu, “Improving glucose oxidase properties by directed evolution,” no. January, 2007.

6. Supplementary material

6.1 Selection of *E. coli* strain for large-scale production

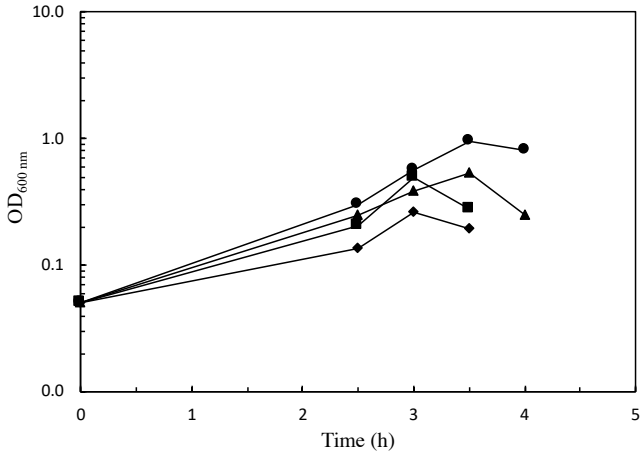

Figure S6.1 Growing curve performed for four distinct growth of BL21 star carrying the wild-type AsP2Ox in large-scale production (1L). Symbols are the values taken by monitoring the optic density at 600 nm. The lines represent the hypothetical grow curve.

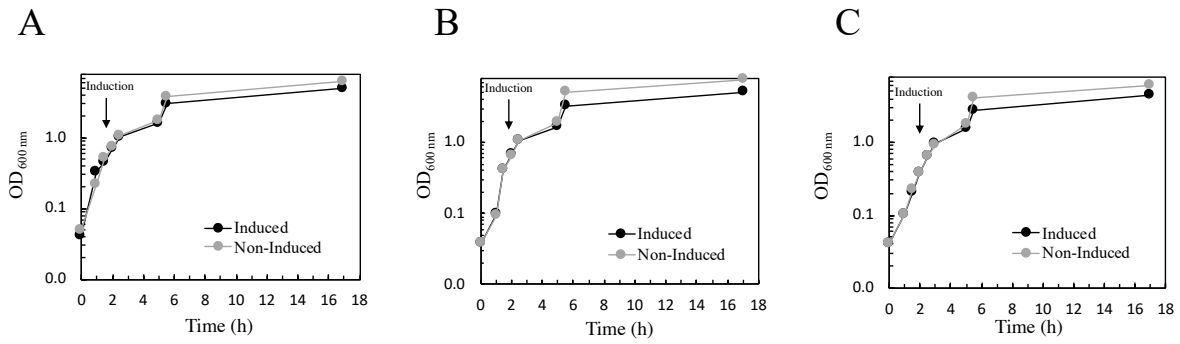

Figure S6.2 Growing curve performed for three distinct *E. coli* strains carrying the wild-type gene of AsP2Ox in small-scale production (50 mL). (A) *E. coli* BL21 star strain; (B) Tuner strain; (C) Rosetta strain. The circle symbols represent the data obtained by monitoring the absorbance at 600 nm. Grey colour represents the data from the non-induced growth of each strain tested and the black colour represent measurements obtained from induced growth with 100 μM of IPTG (the moment of induction of plasmid expression containing the *asp2ox* gene ~0.8 A.U. are marked in each graphic with an arrow).

6.2 Preliminary test of AsP2Ox with B-PER detergent

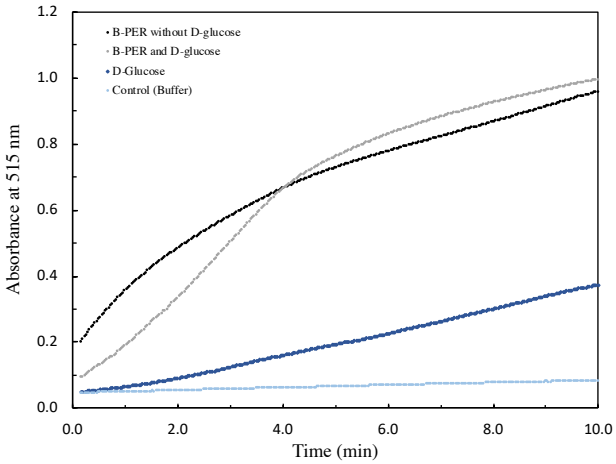

Figure S6.3 Assay to test the B-PER detergent as substrate of AsP2Ox. The assay was performed with pure wild-type AsP2Ox using HRP-AAP/DCHBS as detection method in absence of any electron donor (light blue line), in presence of 1 M of D-glucose (dark blue line), in presence of 10 % B-PER + 1 M of D-glucose (grey line) and in the presence of of 10 % B-PER without D-glucose (black line). The reaction mix contains also 8 U HRP, 1 mM AAP and 10 mM of DCHBS. Assays were performed in 200 μL at 25ºC

6.3 Directed evolution hit variants characterization for O_2

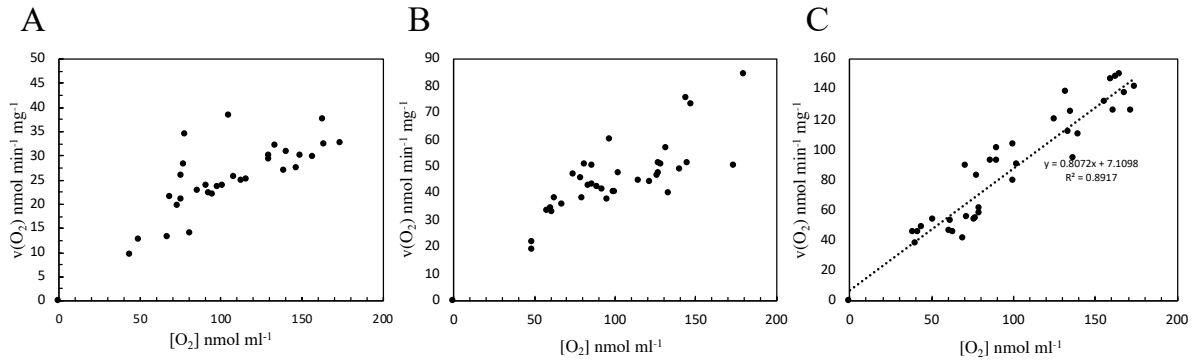

Figure S6.4 Steady-state curves obtained during the Oxygraph assays for the AsP2Ox variants. Data from steady-state following the dioxygen consumption for (A) wild-type, (B) 1A1 variant and (C) 5D5 variant. The rate of consumption of dioxygen was referred as v(O_2). The assays were performed at 37ºC with 1 M of D-glucose in 100 mM sodium phosphates buffer pH 7.5 (for wild-type and 1A1 variant) or in 50 mM Tris-HCl pH 8.5 (for 5D5 variant). For wild-type and 1A1 the steady-state kinetic parameters were calculated using OriginLab by directly fitting of the Michaelis-Menten equation. For 5D5 the catalytic efficiency for O_2 was calculated with the approximation that the [O_2] used was much lower than the K_m ([S]<<K_m).

6.4 SDM mutants steady-state characterization

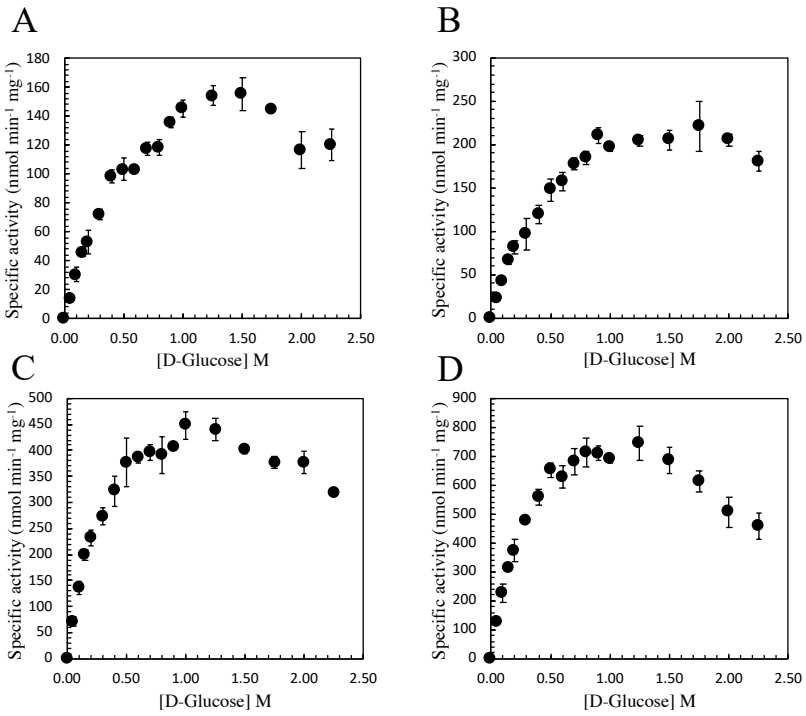

Figure S6.5 Steady-state kinetic curves for the AsP2Ox SDM variants (single and double mutants). Example of steady-state kinetics obtained using the HRP-AAP/DCHBS method of detection for the single mutants (A) A75T, (B) A206T, (C) Q295H and double mutant (D) Q295H/G366S. The assays were performed at 37ºC and the reaction mix contains 0.1 mM of AAP, 1 mM of DCHBS and 8 U of HRP in 100 mM sodium phosphates buffer pH 7.5 (for A75T and A206T mutants) or in 50 mM Tris-HCl pH 8.5 (for Q295H and Q295H/G366S mutants).